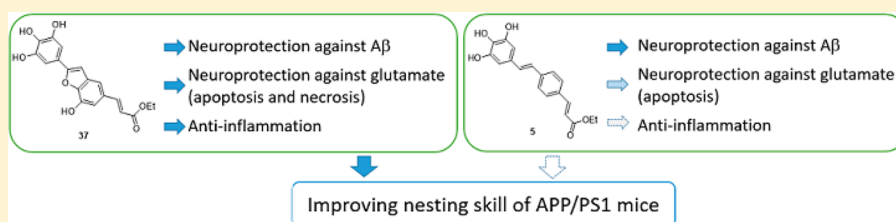


Neuroprotective and Antineuroinflammatory Effects of Hydroxyl-Functionalized Stilbenes and 2-Arylbenzo[*b*]furansPei-Chun Chen,<sup>†</sup> Wei-Jern Tsai,<sup>‡</sup> Yune-Fang Ueng,<sup>‡</sup> Tsai-Teng Tzeng,<sup>†</sup> Hsiang-Ling Chen,<sup>†</sup> Pei-Ru Zhu,<sup>†</sup> Chia-Hsiang Huang,<sup>‡</sup> Young-Ji Shiao,<sup>\*,‡,§</sup> and Wen-Tai Li<sup>\*,‡,§</sup><sup>†</sup>Institute of Biopharmaceutical Science, National Yang-Ming University, Taipei 11221, Taiwan, R.O.C.<sup>‡</sup>National Research Institute of Chinese Medicine, Ministry of Health and Welfare, Taipei 11221, Taiwan, R.O.C.

## Supporting Information



**ABSTRACT:** The drugs currently used to treat Alzheimer's disease (AD) are limited in the benefits they confer, and no medication has been clearly proven to cure or delay the progression of AD. Most candidate AD drugs are meant to reduce the production, aggregation, and toxicity of amyloid  $\beta$  ( $A\beta$ ) or to promote  $A\beta$  clearance. Herein, we demonstrate the efficient synthesis of hydroxyl-functionalized stilbene and 2-arylbenzo[*b*]furan derivatives and report on the neuroprotective and anti-inflammatory effects of these phenolic compounds in vitro and in an animal model. Structure–activity relationships revealed that the presence of an acrylate group on 2-arylbenzo[*b*]furan confers neuroprotective and anti-inflammatory effects. Furthermore, compounds 11 and 37 in this study showed particular potential for development as disease-modifying anti-Alzheimer's drugs, based on their neuroprotective effects on neuron cells, their antineuroinflammatory effects on glial cells, and the ability to ameliorate nesting behavior in APP/PS1 mice. These results indicate that 2-arylbenzo[*b*]furans could be candidate compounds for the treatment of AD.

## INTRODUCTION

Alzheimer's disease (AD) is a common neurodegenerative disorder that leads to cognitive decline, irreversible memory loss, disorientation, and language impairment.<sup>1</sup> The histopathological hallmarks of AD include extracellular amyloid deposition of senile plaques and neurofibrillary tangles in various regions of the brain. Senile plaques are massive extracellular deposits of aggregated amyloid- $\beta$  ( $A\beta$ ) peptides, and neurofibrillary tangles are listed among the neuropathological lesions characterizing AD.<sup>2</sup> The etiology of AD has yet to be fully elucidated; however, it is clear that a number of factors likely play important roles in the development of the disease. These factors include the presence of  $A\beta$  and hyperphosphorylated  $\tau$ -proteins, oxidative stress, and low levels of acetylcholine.<sup>3</sup> The inflammation response triggered by AD has also been shown to induce the production of proinflammatory cytokines (such as IL-1 $\beta$ , TNF $\alpha$ , and IL-6) by microglia and resident astrocytes.<sup>4</sup>

Two classes of drug are currently used to treat AD: acetylcholinesterase inhibitors and *N*-methyl-D-aspartate (NMDA) receptor antagonists.<sup>5</sup> Nonetheless, these drugs confer only limited benefits, and no medication has been clearly proven to cure or delay the progression of AD. Much of the existing research in this field has focused on the discovery of small molecules capable of facilitating the development of novel clinical treatments for AD.<sup>6</sup> Indeed, a number of candidate

drugs are currently undergoing clinical evaluation. Most of these drugs seek to reduce the production, aggregation, and toxicity of  $A\beta$  or to promote  $A\beta$  clearance.<sup>7</sup> However, oxidative stress is among the earliest events in AD pathogenesis, and previous research on free radicals and oxidative stress revealed that oxidative damage is a crucial factor in neuronal degeneration.<sup>8</sup> Furthermore, the interaction between  $A\beta$  and Cu<sup>2+</sup> has been shown to contribute to the production of reactive oxygen species (ROS).<sup>9</sup>

Tournefortic acid B (TAB) and lithospermic acid (LSA) are active components isolated from *Tournefortia sarmentosa* Lam. (Boraginaceae), a medicinal plant commonly used in Taiwan as a detoxicant, anti-inflammatory agent, and promotor of circulation to prevent blood stasis.<sup>10</sup> In previous studies, we demonstrated that TAB and LSA derivatives effectively attenuate neurotoxicity mediated by  $A\beta$ , glutamate, NMDA, and 1-methyl-4-phenylpyridinium. Specifically, TAB and LSA achieve this by abrogating calcium overload in mitochondria and retarding the caspase 8-truncated bid–cytochrome *c* pathway.<sup>11–14</sup> Other polyphenols, such as resveratrol (a natural compound with stilbene structure), have also been studied extensively as anti-AD agents because of their antineuroinflammatory properties and

Received: March 11, 2017

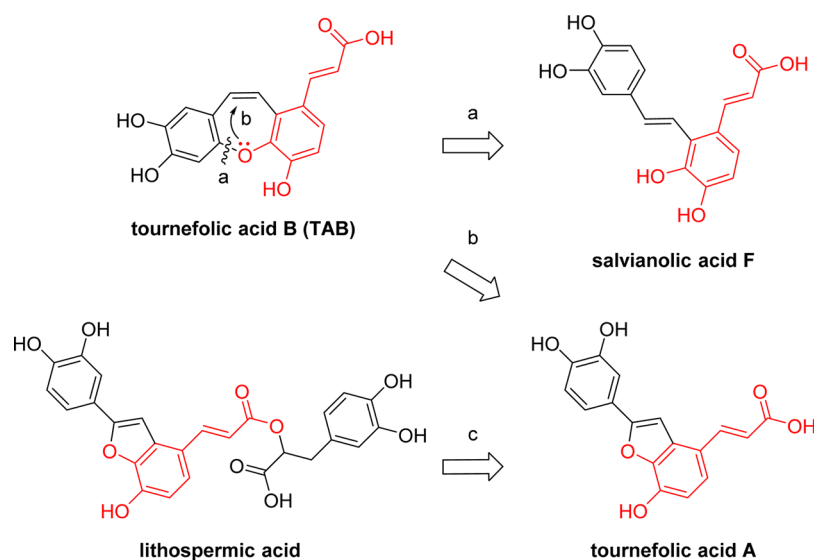
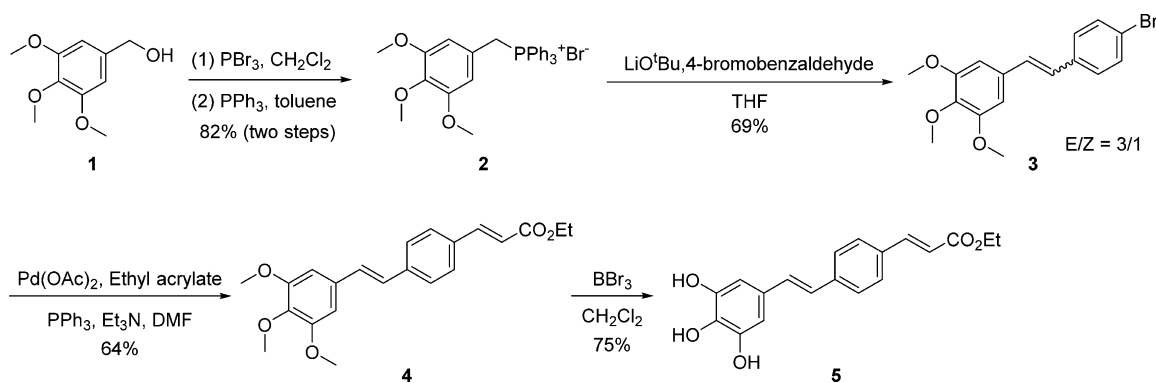
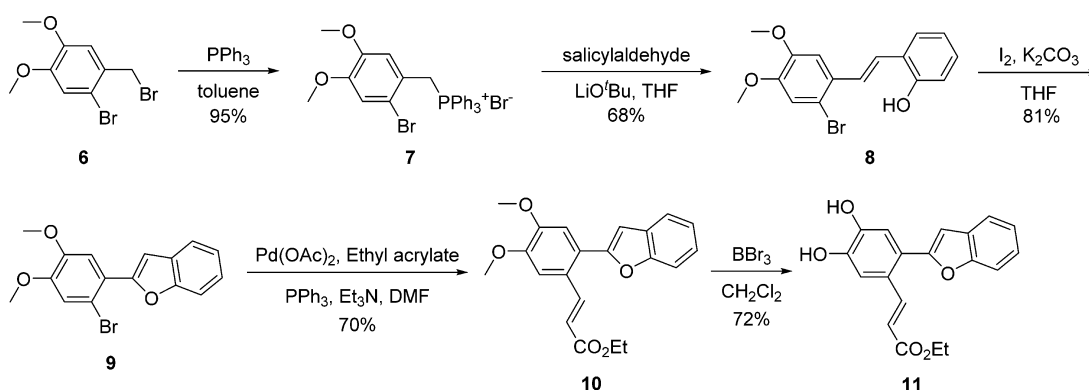


**Figure 1.** Chemical structures of hydroxyl-functionalized tournefoliac acid A and salvianolic acid F, as well as their structural relationships with tournefoliac acid B and lithospermic acid.

### Scheme 1. Synthesis of Hydroxyl-Functionalized Stilbene 5



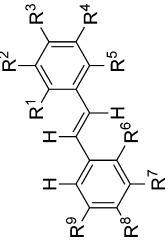
### Scheme 2. Synthesis of Hydroxyl-Functionalized 2-Arylbenzo[*b*]furan 11



ability to inhibit  $A\beta$  aggregation by scavenging oxidants.<sup>15–17</sup> Therefore, we hypothesize that polyphenolic compounds presenting antioxidant activity could form the basis of novel treatments for AD. However, the TAB molecule comprises a seven-membered ring scaffold (belonging to the dibenzoxazepine class), which makes it difficult to synthesize. Nonetheless, the isosteres tournefoliac acid A (TAA) and salvianolic acid F (SAF) are characterized by planar phenolic stilbene and 2-arylbenzo[*b*]furan structures. Because of their antioxidant, anti-inflammatory, and AD-modifying activities, we posit that TAA

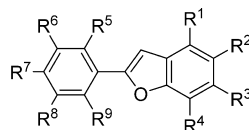
and SAF could potentially be used as starting molecules in the development of novel treatments for AD (Figure 1).<sup>18–22</sup> In the current study, we demonstrate the efficient synthesis of hydroxyl-functionalized stilbene and 2-arylbenzo[*b*]furan derivatives. We also report on the neuroprotective and anti-inflammatory effects of these planar phenolic compounds *in vitro* and in an animal model. We hypothesize that hydroxyl-functionalized stilbenes and 2-arylbenzo[*b*]furans could be a useful starting point for the future development of treatments for AD.

Table 1. Hydroxyl-Functionalized Stilbenes for Neuroprotective and Antineuroinflammatory Effects



compound	R <sup>1</sup>	R <sup>2</sup>	R <sup>3</sup>	R <sup>4</sup>	R <sup>5</sup>	R <sup>6</sup>	R <sup>7</sup>	R <sup>8</sup>	R <sup>9</sup>
4	H	H	CH=CHCO <sub>2</sub> Et <sup>a</sup>	H	H	H	OCH <sub>3</sub>	OCH <sub>3</sub>	OCH <sub>3</sub>
5	H	H	CH=CHCO <sub>2</sub> Et <sup>a</sup>	H	H	H	OH	OH	OH
12	H	H	H	OCH <sub>3</sub>	OH	Br	H	OCH <sub>3</sub>	OCH <sub>3</sub>
13	H	H	H	OCH <sub>3</sub>	OCH <sub>3</sub>	H	H	-OCH <sub>2</sub> O-	-OCH <sub>2</sub> O-
14	H	OCH <sub>3</sub>	OCH <sub>3</sub>	OCH <sub>3</sub>	H	CH=CHCO <sub>2</sub> Et <sup>a</sup>	H	OCH <sub>3</sub>	OCH <sub>3</sub>
15	H	Br	H	OCH <sub>3</sub>	OH	Br	H	OCH <sub>3</sub>	OCH <sub>3</sub>
16	CH=CHCO <sub>2</sub> Et <sup>a</sup>	H	H	OCH <sub>3</sub>	OH	H	H	OCH <sub>3</sub>	OCH <sub>3</sub>
17	CH=CHCO <sub>2</sub> Et <sup>a</sup>	H	H	OCH <sub>3</sub>	OH	H	H	OCH <sub>3</sub>	OCH <sub>3</sub>
18	H	CH=CHCO <sub>2</sub> Et <sup>a</sup>	H	OCH <sub>3</sub>	OH	H	H	OCH <sub>3</sub>	OCH <sub>3</sub>
19	H	H	H	OCH <sub>3</sub>	OH	H	H	OCH <sub>3</sub>	OCH <sub>3</sub>
20	H	H	H	H	OH	H	H	OCH <sub>3</sub>	OCH <sub>3</sub>
21	CH=CHCO <sub>2</sub> Et <sup>a</sup>	H	H	OCH <sub>3</sub>	OH	CH=CHCO <sub>2</sub> Et <sup>a</sup>	H	OCH <sub>3</sub>	OCH <sub>3</sub>
22	H	OCH <sub>3</sub>	OCH <sub>3</sub>	OCH <sub>3</sub>	OH	CH=CHCO <sub>2</sub> Et <sup>a</sup>	OCH <sub>3</sub>	OCH <sub>3</sub>	OCH <sub>3</sub>
23	H	H	H	OCH <sub>3</sub>	OH	CH=CHCO <sub>2</sub> Et <sup>a</sup>	H	OCH <sub>3</sub>	OCH <sub>3</sub>
24	H	H	H	CH=CHCO <sub>2</sub> Et <sup>a</sup>	H	H	H	OH	OH
25	H	H	H	CH=CHCO <sub>2</sub> Et <sup>a</sup>	H	H	H	OCH <sub>3</sub>	OCH <sub>3</sub>
26	H	Br	H	OCH <sub>3</sub>	OH	H	H	OCH <sub>3</sub>	OCH <sub>3</sub>
27	H	H	OCH <sub>3</sub>	H	H	CH=CHCO <sub>2</sub> Et <sup>a</sup>	H	OCH <sub>3</sub>	OCH <sub>3</sub>
28	H	H	OCH <sub>3</sub>	H	H	CH=CHCO <sub>2</sub> Et <sup>a</sup>	H	OCH <sub>3</sub>	OCH <sub>3</sub>
29	H	Br	H	OCH <sub>3</sub>	OH	H	H	OCH <sub>3</sub>	OCH <sub>3</sub>
30	H	H	H	H	OH	Br	H	OCH <sub>3</sub>	OCH <sub>3</sub>
31	H	H	H	OCH <sub>3</sub>	OH	H	H	OCH <sub>3</sub>	OCH <sub>3</sub>
32	H	H	OCH <sub>3</sub>	OH	H	H	H	OCH <sub>3</sub>	OCH <sub>3</sub>
33	H	OCH <sub>3</sub>	OCH <sub>3</sub>	OCH <sub>3</sub>	H	H	H	OCH <sub>3</sub>	OCH <sub>3</sub>
34	H	CHO	H	OCH <sub>3</sub>	OH	H	H	OCH <sub>3</sub>	OCH <sub>3</sub>
35	H	CH=CHCO <sub>2</sub> Me <sup>a</sup>	H	OCH <sub>3</sub>	OH	H	H	OCH <sub>3</sub>	OCH <sub>3</sub>

<sup>a</sup>E isomer.

Table 2. Hydroxyl-Functionalized 2-Arylbenzo[*b*]furans for Neuroprotective and Antineuroinflammatory Effects

compound	R <sup>1</sup>	R <sup>2</sup>	R <sup>3</sup>	R <sup>4</sup>	R <sup>5</sup>	R <sup>6</sup>	R <sup>7</sup>	R <sup>8</sup>	R <sup>9</sup>
11	H	H	H	H	H	OH	OH	H	CH=CHCO <sub>2</sub> Et <sup>a</sup>
36	Br	H	H	OCH <sub>3</sub>	H	-OCH <sub>2</sub> O-		H	H
37	H	CH=CHCO <sub>2</sub> Et <sup>a</sup>	H	OH	H	OH	OH	OH	H
38	H	H	H	H	H	OH	OH	OH	Br
39	H	Br	H	OH	H	OH	OH	OH	H
40	H	Br	H	OH	H	OH	OH	H	H
41	H	Br	H	OH	H	H	OH	H	H
42	Br	H	H	OH	H	H	OH	OH	H
43	H	H	H	OH	H	OH	OH	H	CH=CHCO <sub>2</sub> Et <sup>a</sup>

<sup>a</sup>*E* isomer.

## CHEMISTRY

Schemes 1 and 2 present the strategies used to synthesize novel neuroprotective agents with a structural scaffold composed of hydroxyl-functionalized stilbene and 2-arylbenzo[*b*]furan derivatives. The series of hydroxyl-functionalized stilbene derivatives was synthesized using the following method. First, trimethoxybenzyl alcohol **1** was brominated with phosphorus tribromide to produce trimethoxybenzyl bromide. Then, trimethoxybenzyl bromide was reacted with triphenyl phosphine to produce trimethoxybenzyl phosphorus ylide **2**.<sup>21,23</sup> Subsequently, a Wittig reaction involving 4-bromobenzaldehyde and phosphorus ylide **2** was performed, resulting in the formation of stilbene **3** with a selectivity of approximately *E/Z* = 3/1. The *E* configuration of bromo-substituted stilbene **3** was then coupled with ethyl acrylate via a palladium-catalyzed Heck coupling reaction to produce (*E*)-ethyl acrylate substituted stilbene **4**. Finally, the methoxyl groups were deprotected from compound **4** using boron tribromide to obtain the desired hydroxyl-functionalized stilbene **5** (Scheme 1).

Similarly, 2-arylbenzo[*b*]furan **9** was prepared using the Wittig reaction to convert substituted phosphonium ylide **7** and salicylaldehyde into stilbene **8**. Stilbene **8** was subsequently cyclized in a basic iodine solution to obtain bromo-substituted 2-arylbenzo[*b*]furan **9**, as shown in Scheme 2. The bromo-substituted 2-arylbenzo[*b*]furan **9** was then coupled with ethyl acrylate via a palladium-catalyzed Heck coupling reaction to produce (*E*)-ethyl acrylate substituted 2-arylbenzo[*b*]furan **10**. Finally, the methoxyl groups were removed from compound **10** using the boron tribromide treatment described in Scheme 1 in order to obtain a satisfactory yield of hydroxyl-functionalized 2-arylbenzo[*b*]furan **11**.<sup>21</sup>

## RESULTS

**Hydroxyl-Functionalized Stilbene and 2-Arylbenzo[*b*]furan Derivatives Confer Protective Effects on Cortical Neurons by Reducing  $\text{fA}\beta_{25-35}$ - and Glutamate-Mediated Neurotoxicity.** The maximum nontoxic concentration of each synthesized hydroxyl-functionalized stilbene and 2-arylbenzo[*b*]furan was determined before further analyses were performed. (For details regarding these determinations, refer to Table S1 in the Supporting Information.) Upon so doing, the synthesized hydroxyl-functionalized stilbenes and 2-arylbenzo[*b*]furans were evaluated for neuroprotective effects against fibril amyloid  $\beta$  protein 25–35 ( $\text{fA}\beta_{25-35}$ )- or

glutamate-mediated neurotoxicity, in accordance with standard procedures (Tables 1 and 2). Specifically, the cell viability of neurons was assessed using 3-(4,5-dimethylthiazol-2-yl)-2,5-diphenyl tetrazolium bromide (MTT) reduction analysis. We determined that 5 of the 34 hydroxyl-functionalized stilbenes and 2-arylbenzo[*b*]furans conferred neuroprotective effects against  $\text{fA}\beta_{25-35}$ -mediated toxicity (Tables 3 and 4 and Figure S1). Among those 5 neuroprotective compounds, 3 also presented neuroprotective activities against glutamate-mediated excitotoxicity.

Compounds **5**, **11**, and **37** (all of which are hydroxyl-functionalized stilbene and benzo[*b*]furan derivatives) were shown to confer potent protective benefits on cortical neurons by reducing  $\text{fA}\beta_{25-35}$ - or glutamate-mediated neurotoxicity. Specifically, compounds **5**, **11**, and **37** decreased  $\text{fA}\beta_{25-35}$ -mediated cell death (Table 3 and Figure S1A). Cortical neurons were treated with either vehicle (0.1% DMSO, v/v) or one of the aforementioned compounds at various concentrations. MTT reduction assays revealed that treatment with compounds **5**, **11**, and **37** at 50  $\mu\text{M}$  decreased both  $\text{fA}\beta_{25-35}$ - and glutamate-mediated neuronal death (Table 4 and Figure S1B). Conversely, treatment with compounds **40** and **42** decreased  $\text{A}\beta$ -mediated neuronal death and conferred a moderate protective effect against glutamate-mediated neuronal death. These experiments identified compound **37** as the most effective at protecting neurons against  $\text{fA}\beta_{25-35}$ - and glutamate-mediated toxicity (Table 4).

The live/dead cell viability assay indicated that 10  $\mu\text{M}$   $\text{fA}\beta_{25-35}$  induced a 40% decrease in calcein staining (in terms of both cell number and fluorescence intensity) (Figure 2). However, when cells were treated with 50  $\mu\text{M}$  of compounds **5**, **11**, **37**, **40**, or **42**, the  $\text{fA}\beta_{25-35}$ -induced decrease in calcein staining was significantly attenuated. Conversely, treatment with 30  $\mu\text{M}$  glutamate induced a 50% decrease in calcein staining (in terms of both cell number and fluorescence intensity); however, treatment with 50  $\mu\text{M}$  of compounds **5**, **11**, or **37** significantly attenuated the decrease in calcein staining.

The  $\text{fA}\beta_{25-35}$ -induced cell death was shown to coincide with a 44% reduction in MAP2 and a 36% reduction in tau protein. Compounds **40** and **42** significantly attenuated the decrease in MAP2 (Figure 3A,C); however, none of these six compounds attenuated the decrease in tau protein (Figure 3A,D). Glutamate provoked a decrease in the immunoreactivity of MAP2 (49%) and tau (81%).  $\text{A}\beta$  was also shown to

**Table 3. Neuroprotective and Anti-inflammatory Activities of Hydroxyl-Functionalized Stilbenes and 2-Arylbenzo[*b*]furans on Cortical Neurons and Mixed Glial Culture<sup>a</sup>**

compound	A $\beta$ -mediated neuronal death (%) <sup>b</sup>	Glu-mediated neuronal death (%) <sup>b</sup>	LPS-induced glial NO production (% of vehicle) <sup>b</sup>
vehicle	39.20 $\pm$ 0.88	41.22 $\pm$ 3.40	100
TAB	24.66 $\pm$ 6.31***	42.43 $\pm$ 5.02	98.77 $\pm$ 9.32
TABM	40.12 $\pm$ 7.23	20.38 $\pm$ 9.20***	99.63 $\pm$ 7.55
4	44.43 $\pm$ 4.65	44.56 $\pm$ 2.93	91.44 $\pm$ 16.18
5	19.23 $\pm$ 4.66***	28.05 $\pm$ 3.40**	72.93 $\pm$ 12.67*
11	25.45 $\pm$ 6.14***	21.00 $\pm$ 0.89**	49.61 $\pm$ 7.04*
12	39.67 $\pm$ 0.84	42.89 $\pm$ 2.38	102.71 $\pm$ 3.44
13	38.18 $\pm$ 0.03	44.02 $\pm$ 1.96	95.92 $\pm$ 2.51
14	41.76 $\pm$ 3.36	43.95 $\pm$ 0.67	127.76 $\pm$ 22.65
15	38.78 $\pm$ 0.74	41.17 $\pm$ 2.40	94.57 $\pm$ 29.33
16	38.07 $\pm$ 1.97	44.30 $\pm$ 0.38	106.26 $\pm$ 2.19
17	38.17 $\pm$ 1.53	49.21 $\pm$ 2.32	70.98 $\pm$ 16.18**
18	39.08 $\pm$ 2.78	41.26 $\pm$ 2.09	139.87 $\pm$ 26.41***
19	41.24 $\pm$ 0.94	42.73 $\pm$ 1.88	89.35 $\pm$ 22.23
20	36.56 $\pm$ 1.28	43.30 $\pm$ 2.09	73.27 $\pm$ 1.36**
21	42.53 $\pm$ 2.89	43.06 $\pm$ 2.32	114.19 $\pm$ 19.73
22	41.59 $\pm$ 6.59	39.47 $\pm$ 5.67	123.48 $\pm$ 29.02
23	41.57 $\pm$ 0.98	41.64 $\pm$ 1.95	75.33 $\pm$ 25.27
24	41.19 $\pm$ 2.36	42.05 $\pm$ 1.37	26.02 $\pm$ 2.39***
25	35.98 $\pm$ 3.64	43.29 $\pm$ 0.88	75.60 $\pm$ 11.13
26	41.50 $\pm$ 0.26	42.09 $\pm$ 3.27	88.34 $\pm$ 14.03
27	41.62 $\pm$ 4.44	37.28 $\pm$ 2.97	74.88 $\pm$ 19.64*
28	36.93 $\pm$ 0.60	41.07 $\pm$ 2.14	59.11 $\pm$ 3.05***
29	45.74 $\pm$ 0.41	45.69 $\pm$ 1.40	48.79 $\pm$ 6.21***
30	37.67 $\pm$ 0.49	47.10 $\pm$ 3.06	105.48 $\pm$ 10.60
31	46.98 $\pm$ 2.17	38.42 $\pm$ 2.63	101.00 $\pm$ 7.00
32	43.51 $\pm$ 1.77	30.94 $\pm$ 1.51	81.35 $\pm$ 13.43
33	45.46 $\pm$ 1.90	36.43 $\pm$ 0.53	83.73 $\pm$ 15.24
34	48.16 $\pm$ 3.08	37.02 $\pm$ 3.31	27.99 $\pm$ 11.95*
36	43.98 $\pm$ 2.86	46.84 $\pm$ 3.52	202.71 $\pm$ 26.3***
37	21.18 $\pm$ 3.17***	24.48 $\pm$ 3.68***	40.35 $\pm$ 19.47**
38	42.34 $\pm$ 1.69	41.89 $\pm$ 1.48	24.92 $\pm$ 7.68***
39	45.80 $\pm$ 1.96	43.67 $\pm$ 1.13	106.67 $\pm$ 9.87
40	16.95 $\pm$ 1.30***	31.45 $\pm$ 2.42	86.85 $\pm$ 6.71
41	30.10 $\pm$ 7.00	33.02 $\pm$ 3.01	101.84 $\pm$ 9.16
42	4.11 $\pm$ 0.13***	40.83 $\pm$ 0.98	61.64 $\pm$ 12.53**
43	31.58 $\pm$ 1.50**	43.50 $\pm$ 1.45	38.13 $\pm$ 11.25***

<sup>a</sup>Cortical neurons were incubated with the vehicle (0.1% DMSO) or with the maximum nontoxic concentration of hydroxyl-functionalized stilbenes and 2-arylbenzo[*b*]furans for 2 h before being exposed to A $\beta$  (10  $\mu$ M) for 48 h or glutamate (30  $\mu$ M) for 24 h. After treating the mixed glial cells with LPS for 48 h, culture medium was collected to determine the nitrite content. <sup>b</sup>Concentration of compounds used to investigate A $\beta$ -mediated neuronal death and LPS-induced glial NO production are listed in Table S1. Results are presented as the mean  $\pm$  SD from three independent experiments. Significant differences between the cell group treated with the vehicle and other groups are indicated as follows: \*,  $p < 0.05$ ; \*\*,  $p < 0.01$ ; and \*\*\*,  $p < 0.001$ .

provoke such a decrease; however, it was less pronounced. Nonetheless, treatment with compounds 5, 11, and 37 significantly attenuated both of these decreases (Figure 3A,E,F).

**Hydroxyl-Functionalized Stilbene and 2-Arylbenzo[*b*]furan Derivatives Show Antioxidant Activities and Confer Anti-inflammatory Effects on a Mixed Glial Culture.** To examine the anti-inflammatory activities of the hydroxyl-functionalized stilbene and 2-arylbenzo[*b*]furan derivatives,

we cultured mixed glial cells for 16 days, at which point microglia exhibited a dendritic cell-like appearance.<sup>24</sup> Glial function was then characterized according to the production of nitric oxide (NO) induced by 100 ng/mL lipopolysaccharides (LPS). Interestingly, we found that the level of LPS-induced NO production depended on the amount of time that elapsed after the medium was refreshed. (For details pertaining to this investigation, refer to Figure S2A.) Thus, the cultures that were activated 1 and 2 days after the medium had been refreshed were respectively used as cell models for screening the promotion and inhibition of NO production. Treatment with 50  $\mu$ M of compounds 18 and 36 was shown to increase NO production by 39 and 90%, respectively, in cultures that were activated 1 day after the medium was refreshed (Figure S2B). Treating cells with 50  $\mu$ M of any other compound led to varying effects on NO production in culture that were activated 2 days after the medium was refreshed (Figure S2C). Table 4 lists (1) EC<sub>50</sub> values that describe the degree to which selected compounds inhibit NO production and (2) the antioxidant capacity of selected compounds as determined by trolox equivalent antioxidant capacity (TEAC).

**In Vitro Pharmacokinetic Studies and Calculated Physicochemical Properties.** A preliminary assessment of the in vitro ADMET for active compounds 5, 11, 37, and 40 was completed prior to performing animal assays. In so doing, we found that CYP3A4 appears to be the most abundant cytochrome P450 isoform in the human liver. To assess potential interactions with CYP3A4 substrates, we sought to determine the effects of hydroxyl-functionalized stilbene (compound 5) and 2-arylbenzo[*b*]furans (compounds 11, 37, and 40) on CYP3A4 activity. We observed that the interaction between CYP3A4 and compound 5 was less pronounced than the interaction between CYP3A4 and compounds 11, 37, and 40 (Table 4). Additionally, we calculated the physicochemical properties of compounds 5, 11, and 37 in order to evaluate their brain penetration capabilities and determine whether they meet the overall pharmacokinetics and toxicological requirements to qualify as a central nervous system drug candidate. Specifically, the physicochemical properties were calculated using QikProp (Table 5), which has proven to be highly effective in designing molecules that maximize brain exposure. The physicochemical properties we considered included lipophilicity, as expressed by the calculated logarithm of the octanol/water partition coefficient (QPlogPo/w), the brain/blood partition coefficient (QPlogBB), Caco-2 cell permeability (QPPCaco), total solvent accessible surface area (SASA), and human oral absorption (HOA). The selected compounds presented an excellent drug-like profile with no violations of either Lipinski's rule of five or Jorgensen's rule of three.

Compounds 5, 11, and 37 were selected for in vivo assays due to their effectiveness in in vitro assays. For these assays, we focused on nesting, as this behavior involves a broad network of brain regions. Results of this investigation showed that APP/PS1 mice had lower nesting scores and less nestlet shredding than did WT mice. Furthermore, APP/PS1 mice treated with compounds 11 and 37 (but not 5) registered higher nesting scores than that treated with vehicle (Figure 4A) and presented more pronounced nestlet shredding (Figure 4B).

## DISCUSSION

In neuroprotection assays, five compounds (5, 11, 37, 40, and 42) were found to protect neurons against A $\beta$ -mediated neurotoxicity. Among these five compounds, three (5, 11, and 37) were also

**Table 4.** Neuroprotective and Anti-inflammatory Activities, Inhibition of CYP3A4, and Antioxidant Capacity of Hydroxyl-Functionalized Stilbenes and 2-Arylbenzo[*b*]furans<sup>a</sup>

compound	A $\beta$ -mediated neuronal death (EC <sub>50</sub> , $\mu$ M)	Glu-mediated neuronal death (EC <sub>50</sub> , $\mu$ M)	LPS-induced glial NO (EC <sub>50</sub> , $\mu$ M)	CYP3A4 inhibition (IC <sub>50</sub> , $\mu$ M)	antioxidant capacity (TEAC, mM)
TAB	35.67 $\pm$ 8.39	n.d.	n.d.	n.d.	1.27 $\pm$ 0.20
TABM	n.d.	>MNTC	n.d.	n.d.	1.48 $\pm$ 0.31
5	40.89 $\pm$ 6.45	>MNTC	99.24 $\pm$ 9.89	36.2 $\pm$ 4.2	0.14 $\pm$ 0.01
11	>MNTC	46.08 $\pm$ 7.36	>MNTC	11.2 $\pm$ 3.6	0.01 $\pm$ 0.01
17	>MNTC	>MNTC	66.96 $\pm$ 17.51	n.d.	n.d.
24	>MNTC	>MNTC	48.94 $\pm$ 14.02	n.d.	n.d.
29	>MNTC	>MNTC	84.81 $\pm$ 4.68	n.d.	n.d.
34	>MNTC	>MNTC	42.95 $\pm$ 5.47	n.d.	n.d.
37	52.95 $\pm$ 6.33	32.99 $\pm$ 5.41	56.60 $\pm$ 11.34	21.7 $\pm$ 2.2	0.94 $\pm$ 0.08
38	>MNTC	>MNTC	39.24 $\pm$ 11.94	n.d.	0.97 $\pm$ 0.06
40	36.45 $\pm$ 7.86	>MNTC	>MNTC	23.5 $\pm$ 4.7	0.06 $\pm$ 0.04
42	26.71 $\pm$ 5.39	>MNTC	>MNTC	n.d.	0.12 $\pm$ 0.13
43	>MNTC	>MNTC	82.55 $\pm$ 19.07	n.d.	0.20 $\pm$ 0.07

<sup>a</sup>Results of this investigation are also expressed as EC<sub>50</sub> values representing the mean  $\pm$  SD of three independent experiments. n.d., not determined. MNTC, maximum nontoxic concentration.

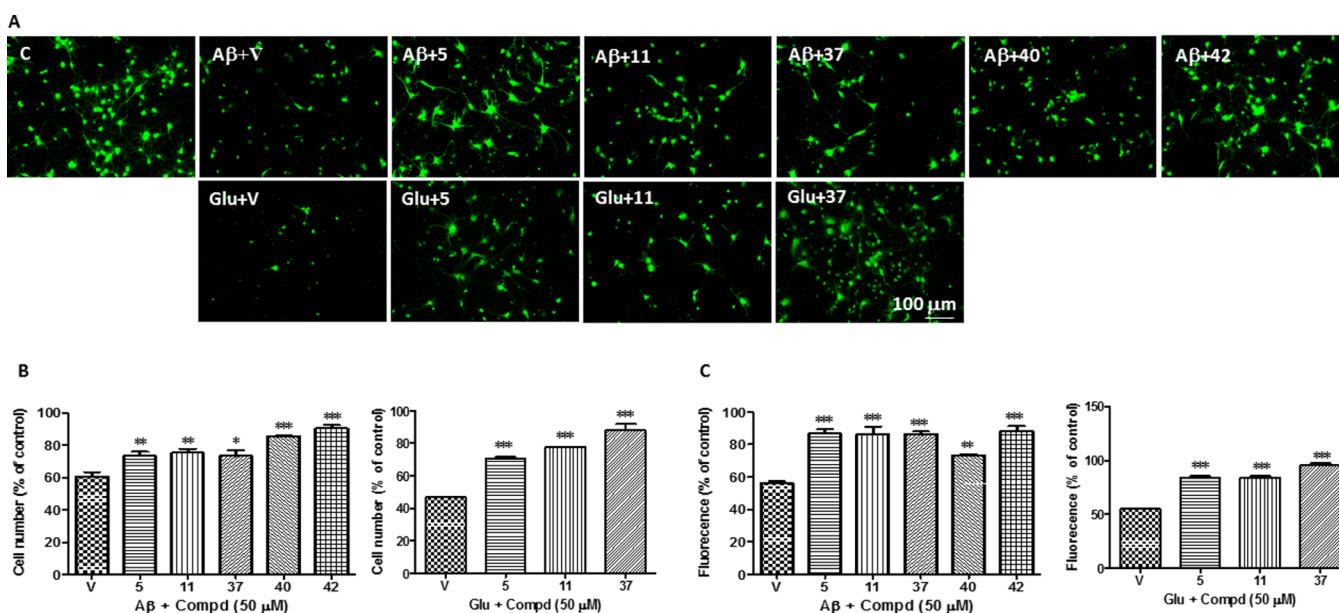


**Figure 2.** Hydroxyl-functionalized stilbene and 2-arylbenzo[*b*]furan protect cortical neurons against A $\beta$ - and glutamate-induced neurite damage. (A) Cortical neurons incubated with 50  $\mu$ M of the indicated compounds for 2 h before being exposed to A $\beta$  (10  $\mu$ M) for 48 h or to glutamate (30  $\mu$ M) for 24 h. (B) Cell viability assessed using the live/dead cell viability assay. The number of live cells was calculated according to the number of calcein AM positive cells. (C) Integrated density of live cells based on the average integrated density of calcein AM positive cells. Results are expressed relative to cells treated with the vehicle alone and represent the mean  $\pm$  SEM from three independent experiments. Significant differences between cells treated with toxin and toxin plus compounds are indicated as follows: \*,  $p$  < 0.05; \*\*,  $p$  < 0.01; and \*\*\*,  $p$  < 0.001.

found to confer protection against glutamate-mediated neurotoxicity. A comparison of compounds with the 3,4,5-trimethoxy ring (4), pyrogallol ring (5), and pyrogallol ring but with acrylate substituted at the R<sup>4</sup> position (24) revealed that compounds 4 and 24 do not confer neuroprotective effects. This suggests that the pyrogallol ring and acrylate substituted at the R<sup>3</sup> position are responsible for the neuroprotective effects of the stilbene scaffold. Moreover, as compared with compound 11, compound 43 was shown to protect neurons against fA $\beta$ 25–35-mediated neurotoxicity, but not against glutamate-mediated neurotoxicity. This suggests that the hydroxyl substitution at the R<sup>4</sup> position of compound 43 counteracts the neuroprotective effects against glutamate-mediated neurotoxicity. In addition, compound 39 differs from compound 37 in that it has a bromide substituent in the R<sup>2</sup> position. This substitution

eliminated the neuroprotective benefits shown by compound 37, which suggests that the acrylate substitution in the R<sup>2</sup> position is responsible for the neuroprotective effects of the 2-arylbenzo[*b*]furan scaffold. Furthermore, unlike compound 40 with the catechol ring on the 2-position of 2-arylbenzo[*b*]furan, pyrogallol ring 39 and 4-hydroxyphenyl ring 41 did not appear to have neuroprotective effects against A $\beta$ -mediated neurotoxicity, which suggests that the catechol ring of 40 is important for this activity. Overall, compounds 5, 11, and 37 were more potent than the reference compounds TAB and TABM against both A $\beta$ - and glutamate-mediated neurotoxicity (Table 3).

In the neurite protection assay, compounds 40 and 42 were shown to protect neurites against A $\beta$ -mediated neurotoxicity, which suggests that the bromo substitution is also important for the protection of neurites (Figure 3). Mixed glial cultures

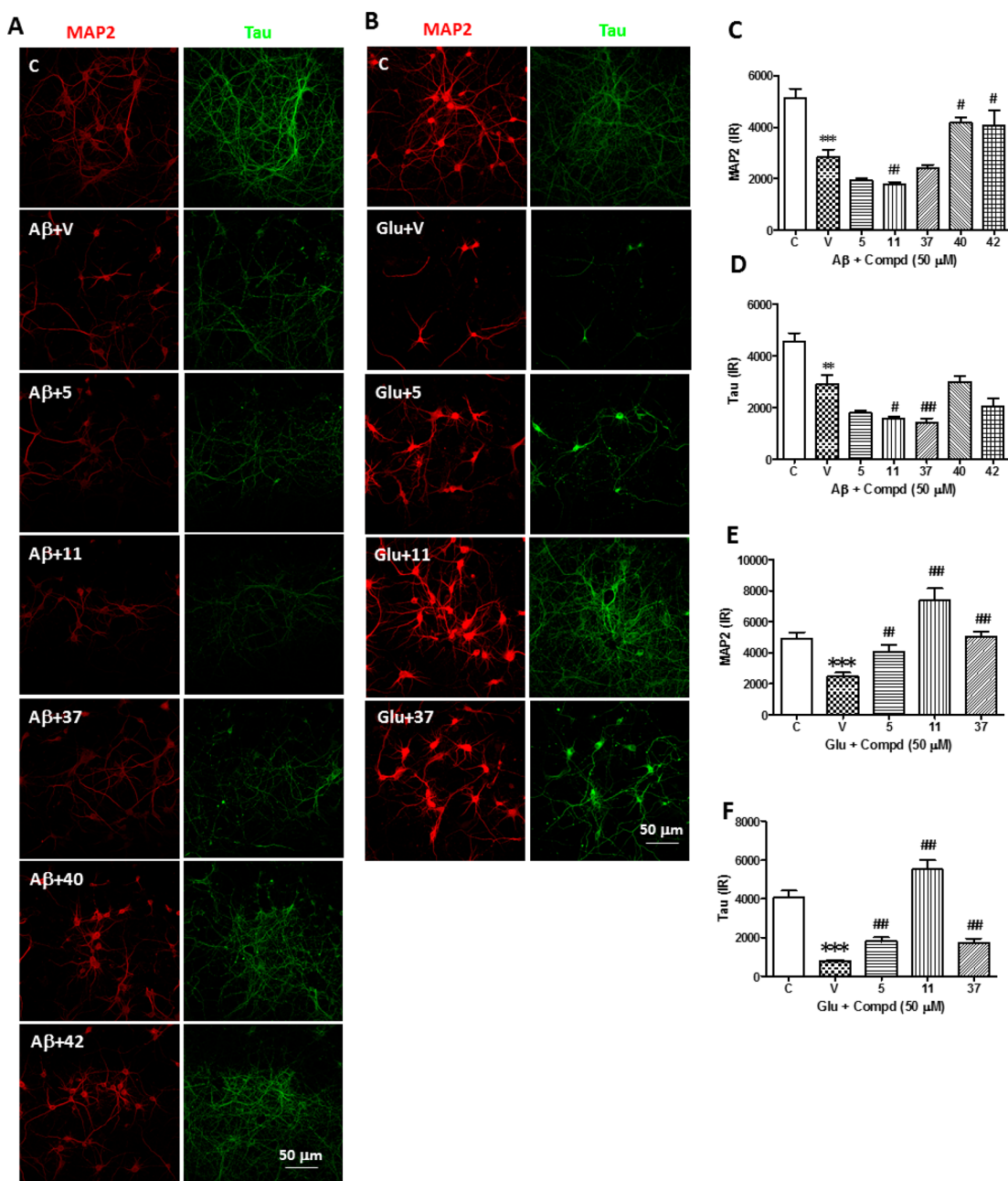


**Figure 3.** Hydroxyl-functionalized stilbene and 2-arylbenzo[*b*]furan protect neurites against  $A\beta$ - and glutamate-induced cell death. Cortical neurons were incubated with  $50 \mu\text{M}$  of the indicated compounds for 2 h before being exposed to either  $10 \mu\text{M}$   $A\beta$  for 48 h (A) or  $30 \mu\text{M}$  glutamate for 24 h (B). (A, B) Representative images showing the immunocytochemistry of MAP2 (red) and tau (green). The integrated density of MAP2 (C, D) and tau protein (E, F) was also measured. Results are expressed relative to cells treated with vehicle alone and represent the mean  $\pm$  SEM from three independent experiments. Significant differences between cells treated with  $A\beta$  and control are indicated as follows: \*\*,  $p < 0.01$ ; \*\*\*,  $p < 0.001$ . Significant differences between cells treated with  $A\beta$  plus vehicle and compounds are indicated as follows: #,  $p < 0.05$ ; ##,  $p < 0.01$ ; and ###,  $p < 0.001$ .

**Table 5.** Calculated Physicochemical Properties for Selected Compounds Using QikProp 2.2<sup>a</sup>

compound	SASA <sup>b</sup>	QPlogPo/w <sup>c</sup>	QlogS <sup>d</sup>	QPlogHERG <sup>e</sup>	QPlogBB <sup>f</sup>	QPCCaco <sup>g</sup>	%HOA <sup>h</sup>
5	655.9	2.95	-4.71	-6.29	-2.2	118.8	81.3
11	583.8	3.19	-4.38	-5.38	-1.2	346.9	91.1
37	652.2	1.88	-4.47	-6.01	-2.6	37.4	66.1

<sup>a</sup>Calculated properties and their recommended range, according to the QikProp user manual. <sup>b</sup>SASA: total solvent accessible surface area in  $\text{\AA}^2$  (300–1000). <sup>c</sup>QPlogPo/w: predicted octanol/water partition coefficient (-2.00 to 6.5). <sup>d</sup>QlogS: predicted aqueous solubility (S in  $\text{mol dm}^{-3}$ ;  $\log S$  -6.5 to 0.5). <sup>e</sup>QPlogHERG: predicted  $\text{IC}_{50}$  value for blockage of HERG  $\text{K}^+$  channels (<-5). <sup>f</sup>QPlogBB: predicted brain/blood partition coefficient (-3.0 to -1.2). <sup>g</sup>QPCCaco: predicted Caco-2 cell permeability in  $\text{nm/s}$  (>500, great; <25%, poor). <sup>h</sup>%HOA: % human oral absorption (>80%, high; <25%, poor).

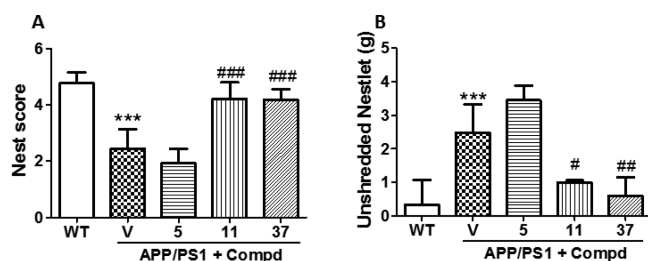


**Figure 4.** Compounds 11 and 37 were shown to restore the negative nesting behavior of APP/PS1 mice. Five-month-old wild type mice were orally administered vehicle (WT), whereas APP/PS1 mice were orally administered vehicle (V) as well as compound 5 (5), 11 (11), or 37 (37) over a period of 60 days before conducting nest construction tests. (A) Nesting scores and (B) the number of unshredded nestlets. The results represent the mean  $\pm$  SD of all WT or APP/PS1 mice. Significant differences between WT and APP/PS1 groups are indicated as follows: \*\*\*,  $p < 0.001$ . Significant differences between compound-treated and control (V) groups are indicated as follows: #,  $p < 0.05$ ; ##,  $p < 0.01$ ; ###,  $p < 0.001$ .

activated by LPS to produce NO were used to evaluate the antineuroinflammatory effects of the compounds.<sup>25,26</sup> Results of this assay revealed that 13 compounds (5, 11, 17, 20, 24, 27, 28, 29, 34, 37, 38, 42, and 43) possessed antineuroinflammatory activities and compounds 24, 34, 37, and 38 were the most active (Tables 3 and 4).

APP/PS1 mice obtained lower nesting scores and presented less nestlet shredding than did WT mice. Nonetheless, compounds 11 or 37 (but not compound 5) were shown to reverse this decline. These results may be due to the fact that compound 5 is a stilbene, whereas 11 and 37 are 2-arylbenzo[*b*]furans. The molecular structure of hydroxyl-functionalized stilbene 5 is close to the naturally occurring polyphenol resveratrol. Resveratrol has a very limited half-life in plasma and poor bioavailability.<sup>27</sup> Therefore, despite the fact that compound 5 was active in all in vitro assays, it may not have been effective in the in vivo assay due to the same issue. Further pharmacokinetic and metabolic studies on these compounds are currently under active investigation and will be reported in due course.

## CONCLUSIONS

Much of the current research aimed at developing therapeutic drugs for AD is based on the hypothesis that A $\beta$  plays a pivotal role in the onset and progression of AD and that the secondary consequences of A $\beta$  generation and deposition (oxidation, inflammation, and excitotoxicity) exacerbate disease progression. This leads to the conclusion that limiting oxidation, excitotoxicity, and inflammation may be beneficial as disease-modifying strategies.<sup>28</sup> In the current study, we demonstrate the efficient synthesis of hydroxyl-functionalized stilbene and 2-arylbenzo[*b*]furan derivatives and report on the neuroprotective and anti-inflammatory effects of these planar phenolic compounds in vitro and in an animal model. Hydroxyl-functionalized stilbenes and 2-arylbenzo[*b*]furans appear to confer neuroprotective effects on neuron cells and antineuroinflammatory effects on glial cells, whereas only 2-arylbenzo[*b*]furans were shown to ameliorate ADL in APP/PS1 mice. Taken together, our findings suggest that hydroxyl-functionalized 2-arylbenzo[*b*]furans could be a useful starting point for future efforts to develop and improve treatments for AD.

## EXPERIMENTAL SECTION

**Compound Synthesis and Characterization.** All reactions were conducted using dried glassware in an oven at 120 °C overnight, after which the samples were underwent cooling in a desiccator. Unless otherwise specified, all reagents were used as received from commercial suppliers. Dichloromethane (DCM) and *N,N'*-dimethylformamide (DMF) were dried over calcium hydride for 48 h prior to distillation. Tetrahydrofuran (THF) was distilled from sodium/benzophenone ketyl under nitrogen. <sup>1</sup>H NMR spectra were obtained using Bruker Avance 400 (400 MHz), Varian Unity Inova 500 (500 MHz), and Varian VNMR600 (600 MHz) spectrometers. All NMR chemical shifts are reported as  $\delta$  values in parts per million (ppm), and coupling constants (*J*) are given in hertz (Hz). The abbreviations of splitting patterns are as follows: singlet (s); doublet (d); triplet (t); quartet (q); broad (br); multiplet that remains unresolved due to the field strength of the instrument (m); doublet of doublets (dd); doublet of triplets (dt); and doublet of doublets of doublets (ddd). Melting points were measured using a Yanaco MP-S3 micro melting point apparatus and are not corrected. Fourier transform infrared spectra were collected using an Avatar 320 spectrometer. Mass spectra and high-resolution mass spectra were recorded on ThermoQuest Finnigan and ThermoQExactive Focus mass spectrometers, respectively. Purification was performed using preparative separations in flash column chromatography (Merck silica gel 60, particle size of 230–400 mesh). Analytical TLC was conducted on precoated plates (Merck silica gel 60, F254). Compounds analyzed on TLC plates were visualized using a UV light, I<sub>2</sub> vapor, or basic aqueous potassium permanganate (KMnO<sub>4</sub>) under heating. All compounds submitted for biological testing were confirmed to be of >95% purity, based on HPLC chromatograms obtained using a Shimadzu VP series HPLC in conjunction with a Shiseido Capcell PAK C18 column (250 mm  $\times$  4.6 mm, 5  $\mu$ m, 1.0 mL/min flow rate).

**General Procedure for the Synthesis of 5-(4-Bromostyryl)-1,2,3-trimethoxybenzene (3) via Wittig Reaction.** A solution of phosphorus ylide 2 (354 mg, 0.68 mmol) in THF (30 mL) was cooled to 0 °C under nitrogen, and lithium *tert*-butoxide (108 mg, 1.35 mmol) was added portionwise. The mixture was stirred at 0 °C for 30 min. A solution of 4-bromobenzaldehyde (126 mg, 0.68 mmol) in THF (7 mL) was added dropwise at 0 °C, and the reaction mixture was warmed to room temperature and stirred for 24 h. Saturated aqueous NH<sub>4</sub>Cl solution was added to the reaction mixture, and the mixture was extracted with EtOAc (20 mL  $\times$  3). The combined organic layers were washed with brine, dried with MgSO<sub>4</sub>, filtered, and concentrated. The residue was purified by silica gel column chromatography to yield 3 (164 mg, 69%, combined yield, *E/Z* = 3/1).

**General Procedure for the Synthesis of Ethyl (E)-3-(4-((E)-3,4,5-Trimethoxystyryl)phenyl)acrylate (4) via Palladium-Catalyzed Coupling Reaction.** A solution of (E)-5-(4-bromostyryl)-1,2,3-trimethoxybenzene 3 (300 mg, 0.86 mmol), ethyl acrylate (0.11 mL, 1.03 mmol), palladium(II) acetate (10 mg, 0.045 mmol), copper(I) iodide (9 mg, 0.045 mmol), and triethylamine (0.24 mL) in *N,N'*-dimethylformamide (10 mL) under a nitrogen atmosphere was heated at 70 °C for 24 h until the reaction was complete, as indicated by TLC. The reaction mixture was quenched with water and extracted with ethyl acetate. The organic layers were combined, dried over MgSO<sub>4</sub>, and concentrated. The residue was purified by column chromatography to give ethyl (E)-3-(4-((E)-3,4,5-trimethoxystyryl)phenyl)acrylate 4 (203 mg, 64%) as a white solid. mp 178–180 °C; <sup>1</sup>H NMR (500 MHz, CDCl<sub>3</sub>):  $\delta$  7.66 (d, *J* = 16.0 Hz, 1H), 7.49 (s, 4H), 7.07 (d, *J* = 16.0 Hz, 1H), 6.98 (d, *J* = 16.0 Hz, 1H), 6.73 (s, 2H), 6.42 (d, *J* = 16.0 Hz, 1H), 4.24 (q, *J* = 7.5 Hz, 2H), 3.90 (s, 6H), 3.86 (s, 3H), 1.32 (t, *J* = 7.5 Hz, 3H); <sup>13</sup>C NMR (125 MHz, CDCl<sub>3</sub>):  $\delta$  167.0, 153.0, 144.0, 139.5, 133.2, 132.2, 131.3, 129.5, 129.1, 127.9, 118.0, 106.1, 60.9, 60.5, 55.9, 14.3; HRMS *m/z* (*M* + 1)<sup>+</sup> calcd for C<sub>22</sub>H<sub>25</sub>O<sub>5</sub>, 369.1697; found, 369.1693.

**General Procedure for the Synthesis of 2-(2-Bromo-4,5-dimethoxyphenyl)benzofuran (9).** A solution of 2-(2-bromo-4,5-dimethoxyphenyl)phenol 8 (241 mg, 0.72 mmol) in 20 mL of THF was mixed with potassium carbonate (594 mg, 4.3 mmol) and iodine (1.09 g, 4.3 mmol). The mixture was stirred at room temperature for 3 h until the reaction was complete, as indicated by TLC.

Saturated NaHSO<sub>3</sub> aqueous solution was added to the solution, and the mixture was extracted with ethyl acetate. The organic layers were combined and dried over MgSO<sub>4</sub>. The residue was purified by flash column chromatography to afford the title compound (194 mg, 81%) as a yellowish solid. <sup>1</sup>H NMR (600 MHz, CDCl<sub>3</sub>): δ 7.60 (d, *J* = 7.8 Hz, 1H), 7.51 (d, *J* = 7.8 Hz, 1H), 7.45 (s, 1H), 7.44 (s, 1H), 7.29 (dt, *J* = 7.8, 1.8 Hz, 1H), 7.23 (dt, *J* = 7.8, 1.8 Hz, 1H), 7.13 (s, 1H), 3.96 (s, 3H), 3.91 (s, 3H); <sup>13</sup>C NMR (150 MHz, CDCl<sub>3</sub>): δ 154.0, 153.2, 149.4, 148.4, 129.0, 124.5, 123.5, 122.9, 121.2, 116.7, 111.9, 111.5, 111.0, 105.9, 56.2, 56.2; HRMS *m/z* (*M* + 1)<sup>+</sup> calcd for C<sub>16</sub>H<sub>14</sub>BrO<sub>3</sub>, 333.0121; found, 333.0119.

**General Procedure for the Synthesis of (E)-Ethyl 3-(2-(benzofuran-2-yl)-4,5-dihydroxyphenyl)acrylate (11).** To a solution of **10** (254 mg, 0.72 mmol) in dry dichloromethane (20 mL) at -60 °C under N<sub>2</sub> was added BBr<sub>3</sub> (0.40 mL, 4.32 mmol) dropwise. The reaction mixture was then allowed to warm to -40 °C and stirred for another 2 h until complete, as indicated by TLC. The reaction was carefully mixed with saturated aqueous NaHCO<sub>3</sub> (30 mL) at 0 °C and stirred for 30 min. This mixture was extracted with ethyl acetate twice (20 mL × 2), and the organic portion was combined, washed further with brine, and dried with MgSO<sub>4</sub>. The residue was filtered, concentrated, and purified by silica gel column chromatography to yield **11** as a white solid (168 mg, 72%). mp 87–89 °C; <sup>1</sup>H NMR (600 MHz, CDCl<sub>3</sub>): δ 8.11 (d, *J* = 16.0 Hz, 1H), 7.58 (dd, *J* = 8.0, 1.2 Hz, 1H), 7.48 (dd, *J* = 8.0, 0.4 Hz, 1H), 7.34 (s, 1H), 7.27 (dt, *J* = 8.0, 0.4 Hz, 1H), 7.22–7.17 (m, 1H), 7.17 (s, 1H), 6.70 (s, 1H), 6.28 (d, *J* = 16.0 Hz, 1H), 5.95 (br, 1H), 5.87 (br 1H), 4.25 (q, *J* = 7.2 Hz, 2H), 1.32 (t, *J* = 7.2 Hz, 3H); <sup>13</sup>C NMR (150 MHz, CDCl<sub>3</sub>): δ 167.3, 154.7, 153.4, 145.4, 144.4, 143.0, 129.1, 126.4, 124.6, 124.5, 123.0, 121.1, 118.6, 115.1, 113.9, 111.1, 106.7, 60.6, 14.3; HRMS *m/z* (*M* - 1)<sup>-</sup> calcd for C<sub>19</sub>H<sub>15</sub>O<sub>5</sub>, 323.0914; found, 323.0918.

**(E)-2-(2-Bromo-4,5-dimethoxystyryl)-6-methoxyphenol (12).** White solid; mp 156–158 °C; <sup>1</sup>H NMR (500 MHz, CDCl<sub>3</sub>): δ 7.00 (s, 1H), 6.75 (d, *J* = 12.0, 1H), 6.72–6.65 (m, 3H), 6.60 (t, *J* = 8.0 Hz, 1H), 5.77 (s, 1H), 3.86 (s, 3H), 3.84 (s, 3H), 3.43 (s, 3H); <sup>13</sup>C NMR (125 MHz, CDCl<sub>3</sub>): δ 148.8, 147.6, 146.6, 143.5, 129.6, 129.5, 124.8, 123.0, 122.1, 119.1, 115.0, 114.4, 113.2, 109.5, 56.0, 56.0, 55.6; HRMS *m/z* (*M* + 1)<sup>+</sup> calcd for C<sub>17</sub>H<sub>13</sub>BrO<sub>4</sub>, 365.0383; found, 365.0378.

**(E)-5-(2,3-Dimethoxystyryl)benzo[d][1,3]dioxole (13).** White solid; mp 143–145 °C; <sup>1</sup>H NMR (500 MHz, CDCl<sub>3</sub>): δ 6.76 (d, *J* = 8.0 Hz, 1H), 6.75–6.72 (m, 1H), 6.68 (d, *J* = 8.0 Hz, 1H), 6.62–6.57 (m, 4H), 6.52 (dd, *J* = 8.0, 2.0 Hz, 1H), 5.88 (s, 2H), 3.84 (s, 3H), 3.82 (s, 3H); <sup>13</sup>C NMR (125 MHz, CDCl<sub>3</sub>): δ 147.3, 145.8, 131.1, 129.9, 129.3, 125.3, 123.5, 121.9, 121.6, 111.2, 109.9, 109.5, 109.2, 108.1, 100.8, 60.8, 55.7; HRMS *m/z* (*M* + 1)<sup>+</sup> calcd for C<sub>17</sub>H<sub>17</sub>O<sub>4</sub>, 285.1121; found, 285.1117.

**Ethyl (E)-3-(6-((E)-3,4,5-Trimethoxystyryl)benzo[d][1,3]dioxol-5-yl)acrylate (14).** Yellow solid; mp 123–125 °C; <sup>1</sup>H NMR (600 MHz, CDCl<sub>3</sub>): δ 8.04 (d, *J* = 15.6 Hz, 1H), 7.27 (d, *J* = 15.6 Hz, 1H), 7.03 (d, *J* = 6.6 Hz, 1H), 6.77 (d, *J* = 16.2 Hz, 1H), 6.71 (s, 2H), 6.23 (d, *J* = 15.6 Hz, 1H), 6.00 (s, 2H), 4.23 (q, *J* = 7.2 Hz, 2H), 3.90 (s, 6H), 3.85 (s, 3H), 1.31 (t, *J* = 7.2 Hz, 3H); <sup>13</sup>C NMR (125 MHz, CDCl<sub>3</sub>): δ 167.1, 153.4, 149.7, 147.8, 141.5, 138.2, 133.1, 132.9, 131.5, 126.8, 124.6, 118.1, 106.3, 106.0, 103.8, 101.6, 61.0, 60.5, 56.2, 14.3; HRMS *m/z* (*M* + 1)<sup>+</sup> calcd for C<sub>23</sub>H<sub>25</sub>O<sub>7</sub>, 413.1595; found, 413.1586.

**(E)-Ethyl 3-(2-((E)-3,4-Dimethoxystyryl)-3-hydroxy-4-methoxyphenyl)acrylate (16).** White solid; mp 108–112 °C; <sup>1</sup>H NMR (500 MHz, CDCl<sub>3</sub>): δ 8.01 (d, *J* = 15.5 Hz, 1H), 7.14 (d, *J* = 8.5 Hz, 1H), 7.13 (d, *J* = 16.5 Hz, 1H), 7.07–7.04 (m, 2H), 6.88 (d, *J* = 16.5 Hz, 1H), 6.83 (d, *J* = 8.0 Hz, 1H), 6.78 (d, *J* = 8.5 Hz, 1H), 6.27 (d, *J* = 16.0 Hz, 1H), 4.22 (q, *J* = 7.0 Hz, 2H), 3.93 (s, 3H), 3.92 (s, 3H), 3.89 (s, 3H), 1.27 (t, *J* = 7.0 Hz, 3H); <sup>13</sup>C NMR (125 MHz, CDCl<sub>3</sub>): δ 167.1, 149.1, 149.0, 147.4, 143.8, 143.5, 136.4, 130.7, 127.0, 124.7, 120.1, 119.4, 119.3, 118.0, 11.1, 109.2, 109.0, 60.3, 56.2, 56.0, 55.9, 14.3; HRMS *m/z* (*M* + 1)<sup>+</sup> calcd for C<sub>22</sub>H<sub>25</sub>O<sub>6</sub>, 385.1646; found, 385.1642.

**Ethyl (E)-3-(2-((E)-2-(Benzo[d][1,3]dioxol-5-yl)vinyl)-3-hydroxy-4-methoxyphenyl)acrylate (17).** Yellow solid; mp 168–170 °C; <sup>1</sup>H NMR (500 MHz, CDCl<sub>3</sub>): δ 8.00 (d, *J* = 16.0 Hz, 1H), 7.12 (d, *J* = 8.0 Hz, 1H), 7.09 (d, *J* = 16.0 Hz, 1H), 7.08 (d, *J* = 1.5 Hz, 1H),

7.07 (d, *J* = 1.5 Hz, 1H), 6.93 (dd, *J* = 8.0, 1.5 Hz, 1H), 6.86 (d, *J* = 16.0 Hz, 1H), 6.77 (dd, *J* = 8.0, 1.5 Hz, 1H), 6.25 (d, *J* = 16.0 Hz, 1H), 6.00 (s, 1H), 5.95 (s, 2H), 4.23 (q, *J* = 7.0 Hz, 2H), 3.90 (s, 3H), 1.30 (t, *J* = 7.0 Hz, 3H); <sup>13</sup>C NMR (125 MHz, CDCl<sub>3</sub>): δ 167.1, 148.1, 147.5, 147.4, 143.8, 143.5, 136.1, 132.1, 127.0, 124.5, 121.7, 119.5, 119.4, 118.0, 109.2, 108.3, 105.7, 101.1, 60.3, 56.1, 14.3; HRMS *m/z* (*M* + 1)<sup>+</sup> calcd for C<sub>21</sub>H<sub>21</sub>O<sub>6</sub>, 369.1333; found, 369.1326.

**Ethyl (E)-3-(2-((E)-2-(Benzo[d][1,3]dioxol-5-yl)vinyl)-4-hydroxy-5-methoxyphenyl)acrylate (18).** Yellow solid; mp 155–157 °C; <sup>1</sup>H NMR (500 MHz, CDCl<sub>3</sub>): δ 7.63 (d, *J* = 15.5 Hz, 1H), 7.32 (d, *J* = 1.5 Hz, 1H), 7.19 (d, *J* = 16.5 Hz, 1H), 7.10 (d, *J* = 16.5 Hz, 1H), 7.09 (d, *J* = 1.5 Hz, 1H), 6.95 (dd, *J* = 8.0, 1.5 Hz, 1H), 6.92 (d, *J* = 1.5 Hz, 1H), 6.78 (d, *J* = 8.0 Hz, 1H), 6.32 (d, *J* = 16.0 Hz, 1H), 6.14 (s, 1H), 5.96 (s, 1H), 4.25 (d, *J* = 7.5 Hz, 2H), 3.93 (s, 3H), 1.32 (t, *J* = 7.5 Hz, 3H); <sup>13</sup>C NMR (125 MHz, CDCl<sub>3</sub>): δ 167.2, 148.1, 147.4, 146.9, 145.3, 144.8, 135.2, 135.1, 132.1, 130.4, 129.9, 127.9, 126.4, 124.0, 121.7, 120.4, 120.2, 115.9, 108.4, 107.5, 105.7, 101.1, 60.4, 56.2, 14.4; HRMS *m/z* (*M* + 1)<sup>+</sup> calcd for C<sub>21</sub>H<sub>21</sub>O<sub>6</sub>, 369.1333; found, 369.1327.

**(E)-Ethyl 3-(2-((E)-2-Hydroxy-3-methoxystyryl)-4,5-dimethoxyphenyl)acrylate (19).** Amorphous powder; <sup>1</sup>H NMR (500 MHz, CDCl<sub>3</sub>): δ 8.10 (d, *J* = 16.0 Hz, 1H), 7.53 (d, *J* = 16.0 Hz, 1H), 7.19 (d, *J* = 16.0 Hz, 1H), 7.16 (dd, *J* = 8.0, 1.0 Hz, 1H), 7.10 (s, 1H), 7.02 (s, 1H), 6.84 (t, *J* = 8.0 Hz, 1H), 6.77 (dd, *J* = 8.5, 1.5 Hz, 1H), 6.27 (d, *J* = 16.0 Hz, 1H), 6.01 (s, 1H), 4.25 (q, *J* = 7.5 Hz, 2H), 3.95 (s, 3H), 3.90 (s, 3H), 3.89 (s, 3H), 1.32 (t, *J* = 7.5 Hz, 3H); <sup>13</sup>C NMR (125 MHz, CDCl<sub>3</sub>): δ 167.2, 150.9, 148.8, 146.7, 143.5, 141.8, 132.1, 125.9, 125.3, 125.3, 123.6, 119.6, 119.1, 117.6, 109.7, 108.8, 108.8, 60.4, 56.1, 56.0, 55.9; HRMS *m/z* (*M* + 1)<sup>+</sup> calcd for C<sub>22</sub>H<sub>25</sub>O<sub>6</sub>, 385.1646; found, 385.1638.

**Ethyl (E)-3-(2-((E)-2-Hydroxystyryl)-4,5-dimethoxyphenyl)acrylate (20).** Yellow solid; mp 158–161 °C; <sup>1</sup>H NMR (500 MHz, CDCl<sub>3</sub>): δ 8.10 (d, *J* = 16.2 Hz, 1H), 7.52 (dd, *J* = 7.8, 1.8 Hz, 1H), 7.45 (d, *J* = 16.2 Hz, 1H), 7.14 (dt, *J* = 7.8, 1.8 Hz, 1H), 7.13 (d, *J* = 16.2 Hz, 1H), 7.07 (s, 1H), 7.03 (s, 1H), 6.94 (dt, *J* = 7.8, 1.2 Hz, 1H), 6.79 (dd, *J* = 8.4, 1.2 Hz, 1H), 6.27 (d, *J* = 16.2 Hz, 1H), 4.25 (q, *J* = 7.2 Hz, 2H), 3.95 (s, 3H), 3.91 (s, 3H), 1.32 (t, *J* = 7.2 Hz, 3H); <sup>13</sup>C NMR (125 MHz, CDCl<sub>3</sub>): δ 167.3, 153.1, 150.1, 148.9, 141.9, 131.9, 128.9, 127.5, 126.5, 125.7, 125.4, 124.6, 121.2, 117.7, 116.0, 109.0, 108.8, 60.5, 56.0, 56.0, 14.4; HRMS *m/z* (*M* + 1)<sup>+</sup> calcd for C<sub>21</sub>H<sub>23</sub>O<sub>5</sub>, 355.1540; found, 355.1533.

**(E)-Ethyl 3-(3-Hydroxy-4-methoxy-2-((E)-3,4,5-trimethoxystyryl)phenyl)acrylate (21).** White solid; mp 174–176 °C; <sup>1</sup>H NMR (500 MHz, CDCl<sub>3</sub>): δ 8.00 (d, *J* = 16.0 Hz, 1H), 7.15 (d, *J* = 16.5 Hz, 1H), 7.11 (d, *J* = 8.5 Hz, 1H), 6.85 (d, *J* = 16.5 Hz, 1H), 6.77 (d, *J* = 8.5 Hz, 1H), 6.72 (s, 1H), 6.27 (d, *J* = 16.0 Hz, 1H), 6.08 (s, 1H), 4.21 (q, *J* = 7.5 Hz, 2H), 3.88 (s, 3H), 3.87 (s, 3H), 3.84 (s, 3H), 1.27 (t, *J* = 7.5 Hz, 3H); <sup>13</sup>C NMR (125 MHz, CDCl<sub>3</sub>): δ 167.0, 153.2, 147.4, 143.7, 143.6, 138.1, 136.3, 133.3, 126.9, 124.3, 120.8, 119.4, 118.0, 109.3, 103.7, 60.8, 60.2, 56.0, 56.0, 14.5; HRMS *m/z* (*M* + 1)<sup>+</sup> calcd for C<sub>23</sub>H<sub>27</sub>O<sub>7</sub>, 415.1751; found, 415.1747.

**(E)-Ethyl 3-(4,5-Dimethoxy-2-((E)-3,4,5-trimethoxystyryl)phenyl)acrylate (22).** White solid; mp 116–118 °C; <sup>1</sup>H NMR (500 MHz, CDCl<sub>3</sub>): δ 7.83 (d, *J* = 16.0 Hz, 1H), 7.04 (s, 1H), 6.70 (s, 1H), 6.67 (d, *J* = 12.0 Hz, 1H), 6.62 (d, *J* = 12.0 Hz, 1H), 6.31 (s, 1H), 6.18 (d, *J* = 16.0 Hz, 1H), 4.18 (q, *J* = 7.0 Hz, 2H), 3.87 (s, 3H), 3.75 (s, 3H), 3.70 (s, 3H), 3.58 (s, 6H), 1.28 (t, *J* = 7.0 Hz, 3H); <sup>13</sup>C NMR (125 MHz, CDCl<sub>3</sub>): δ 167.0, 152.7, 150.6, 148.4, 142.3, 137.3, 132.2, 132.1, 131.8, 127.1, 125.4, 116.9, 112.2, 108.5, 106.3, 60.8, 60.3, 55.9, 55.8, 55.8, 14.3; HRMS *m/z* (*M* + 1)<sup>+</sup> calcd for C<sub>24</sub>H<sub>29</sub>O<sub>7</sub>, 429.1908; found, 429.1902.

**Ethyl (E)-3-(6-((E)-2-Hydroxy-3-methoxystyryl)benzo[d][1,3]dioxol-5-yl)acrylate (23).** White solid; mp 168–170 °C; <sup>1</sup>H NMR (500 MHz, CDCl<sub>3</sub>): δ 8.08 (d, *J* = 16.0 Hz, 1H), 7.50 (d, *J* = 16.0 Hz, 1H), 7.17 (d, *J* = 16.0 Hz, 1H), 7.15 (dd, *J* = 8.0, 1.0 Hz, 1H), 7.13 (s, 1H), 7.00 (s, 1H), 6.83 (t, *J* = 8.0 Hz, 1H), 6.77 (dd, *J* = 8.0, 1.5 Hz, 1H), 6.22 (d, *J* = 16.0 Hz, 1H), 6.00 (s, 1H), 5.98 (s, 2H), 4.23 (q, *J* = 7.0 Hz, 2H), 3.90 (s, 3H), 1.31 (t, *J* = 7.0 Hz, 3H); <sup>13</sup>C NMR (125 MHz, CDCl<sub>3</sub>): δ 167.2, 149.7, 147.6, 146.7, 143.6, 141.7, 133.8, 126.8, 125.7, 125.7, 123.5, 119.6, 119.2, 117.9, 109.7, 106.2, 105.9,

101.5, 60.4, 56.1, 14.3; HRMS  $m/z$  ( $M + 1$ )<sup>+</sup> calcd for C<sub>21</sub>H<sub>21</sub>O<sub>6</sub>, 369.1333; found, 369.1326.

(*E*)-Ethyl 3-(6-(Benzofuran-2-yl)-2,3,4-trihydroxyphenyl)acrylate (**24**). Yellow solid; mp 168–170 °C; <sup>1</sup>H NMR (500 MHz, CD<sub>3</sub>OD): δ 7.68 (d, *J* = 16.2 Hz, 1H), 7.68 (s, 1H), 7.52 (d, *J* = 7.8 Hz, 1H), 7.43 (d, *J* = 7.8 Hz, 1H), 7.35 (t, *J* = 7.8 Hz, 1H), 7.01 (d, *J* = 16.2 Hz, 1H), 6.89 (d, *J* = 16.2 Hz, 1H), 6.59 (s, 2H), 6.55 (d, *J* = 16.2 Hz, 1H), 4.24 (q, *J* = 7.2 Hz, 2H), 1.33 (t, *J* = 7.2 Hz, 3H); <sup>13</sup>C NMR (125 MHz, CD<sub>3</sub>OD): δ 168.6, 147.1, 146.1, 140.1, 136.1, 134.8, 131.3, 130.3, 129.9, 128.9, 127.5, 127.1, 125.9, 119.2, 107.1, 61.6, 14.6; HRMS  $m/z$  ( $M - 1$ )<sup>-</sup> calcd for C<sub>19</sub>H<sub>17</sub>O<sub>5</sub>, 325.1071; found, 325.1066.

(*E*)-Ethyl 3-(3-((*E*)-3,4,5-Trimethoxystyryl)phenyl)acrylate (**25**). White solid; mp 177–179 °C; <sup>1</sup>H NMR (500 MHz, CDCl<sub>3</sub>): δ 7.68 (d, *J* = 16.2 Hz, 1H), 7.62 (s, 1H), 7.48 (d, *J* = 7.8 Hz, 1H), 7.39 (d, *J* = 7.8 Hz, 1H), 7.34 (t, *J* = 7.8 Hz, 1H), 7.04 (d, *J* = 16.2 Hz, 1H), 6.97 (d, *J* = 16.2 Hz, 1H), 6.72 (s, 2H), 6.46 (d, *J* = 15.6 Hz, 1H), 4.25 (q, *J* = 7.2 Hz, 2H), 3.89 (s, 6H), 3.85 (s, 3H), 1.32 (t, *J* = 7.2 Hz, 3H); <sup>13</sup>C NMR (125 MHz, CDCl<sub>3</sub>): δ 166.8, 153.4, 144.3, 138.1, 137.8, 134.8, 132.6, 129.5, 129.1, 128.0, 127.2, 127.0, 125.9, 118.5, 103.6, 60.9, 60.5, 56.0, 14.2; HRMS  $m/z$  ( $M + 1$ )<sup>+</sup> calcd for C<sub>22</sub>H<sub>25</sub>O<sub>5</sub>, 369.1697; found, 369.1693.

(*E*)-4-Bromo-2-(3,4-dimethoxystyryl)-6-methoxyphenol (**26**). Yellow solid; mp 105–107 °C; <sup>1</sup>H NMR (600 MHz, CDCl<sub>3</sub>): δ 7.29 (d, *J* = 2.4 Hz, 1H), 7.18 (d, *J* = 16.2 Hz, 1H), 7.08–7.04 (m, 3H), 6.85–6.83 (m, 2H), 5.84 (s, 1H), 3.93 (s, 3H), 3.89 (s, 6H); <sup>13</sup>C NMR (150 MHz, CDCl<sub>3</sub>): δ 149.1, 149.0, 147.2, 142.6, 131.6, 130.5, 130.3, 125.5, 121.1, 120.2, 119.6, 112.3, 111.7, 111.2, 108.9, 56.4, 56.0; HRMS  $m/z$  ( $M + 1$ )<sup>+</sup> calcd for C<sub>17</sub>H<sub>18</sub>BrO<sub>4</sub>, 365.0384; found, 365.0379.

Ethyl (*E*)-3-(6-((*E*)-4-Methoxystyryl)benzo[d][1,3]dioxol-5-yl)acrylate (**27**). White solid; mp 84–86 °C; <sup>1</sup>H NMR (600 MHz, CDCl<sub>3</sub>): δ 8.07 (d, *J* = 15.6 Hz, 1H), 7.43 (dd, *J* = 7.2, 2.4 Hz, 2H), 7.25 (d, *J* = 15.6 Hz, 1H), 7.04 (s, 1H), 7.00 (s, 1H), 6.88 (dd, *J* = 7.2, 1.8 Hz, 2H), 6.81 (d, *J* = 15.6 Hz, 1H), 6.22 (d, *J* = 15.6 Hz, 1H), 5.98 (s, 2H), 4.24 (q, *J* = 7.2 Hz, 2H), 3.82 (s, 3H), 1.31 (t, *J* = 7.2 Hz, 3H); <sup>13</sup>C NMR (150 MHz, CDCl<sub>3</sub>): δ 167.2, 159.5, 149.7, 147.5, 141.6, 133.5, 131.0, 130.4, 129.9, 127.9, 126.6, 122.8, 117.9, 114.2, 113.6, 106.0, 105.9, 101.5, 60.4, 55.3, 14.3; HRMS  $m/z$  ( $M + 1$ )<sup>+</sup> calcd for C<sub>21</sub>H<sub>21</sub>O<sub>5</sub>, 353.1384; found, 353.1379.

Ethyl (*E*)-3-(2,3,4-Trimethoxy-6-((*E*)-4-methoxystyryl)phenyl)acrylate (**28**). Yellow solid; mp 83–85 °C; <sup>1</sup>H NMR (600 MHz, CDCl<sub>3</sub>): δ 7.92 (d, *J* = 16.2 Hz, 1H), 7.43 (d, *J* = 6.6 Hz, 2H), 7.16 (d, *J* = 16.2 Hz, 1H), 6.89 (d, *J* = 6.6 Hz, 2H), 6.85 (s, 1H), 6.84 (d, *J* = 16.2 Hz, 1H), 6.40 (d, *J* = 16.2 Hz, 1H), 4.23 (q, *J* = 7.2 Hz, 2H), 3.93 (s, 3H), 3.87 (s, 3H), 3.86 (s, 3H), 3.82 (s, 3H), 1.31 (t, *J* = 7.2 Hz, 3H); <sup>13</sup>C NMR (150 MHz, CDCl<sub>3</sub>): δ 167.7, 159.5, 154.3, 153.2, 141.7, 138.5, 134.7, 131.0, 130.0, 127.9, 124.9, 122.3, 120.3, 114.2, 105.8, 61.0, 60.8, 60.3, 56.0, 55.3, 14.3; HRMS  $m/z$  ( $M + 1$ )<sup>+</sup> calcd for C<sub>23</sub>H<sub>27</sub>O<sub>6</sub>, 399.1802; found, 399.1798.

(*E*)-2-(2-(Benzo[d][1,3]dioxol-5-yl)vinyl)-4-bromo-6-methoxyphenol (**29**). White solid; mp > 250 °C; <sup>1</sup>H NMR (600 MHz, CDCl<sub>3</sub>): δ 7.26 (d, *J* = 2.0 Hz, 1H), 7.14 (d, *J* = 16.5 Hz, 1H), 7.07 (d, *J* = 1.5 Hz, 1H), 7.03 (d, *J* = 16.5 Hz, 1H), 6.93 (dd, *J* = 8.0, 1.5 Hz, 1H), 6.83 (d, *J* = 2.5 Hz, 1H), 6.77 (d, *J* = 8.0 Hz, 1H), 5.95 (s, 2H), 3.88 (s, 3H); <sup>13</sup>C NMR (150 MHz, CDCl<sub>3</sub>): δ 148.1, 147.3, 142.3, 131.9, 130.1, 125.3, 121.8, 121.0, 119.8, 112.4, 111.6, 108.4, 105.7, 101.1, 56.4; HRMS  $m/z$  ( $M - 1$ )<sup>-</sup> calcd for C<sub>16</sub>H<sub>12</sub>BrO<sub>4</sub>, 346.9913; found, 346.9920.

(*E*)-2-(2-Bromo-3,4,5-trimethoxystyryl)phenol (**30**). White solid; mp 147–149 °C; <sup>1</sup>H NMR (600 MHz, CDCl<sub>3</sub>): δ 7.54 (dd, *J* = 7.5, 1.5 Hz, 1H), 7.44 (d, *J* = 16.0 Hz, 1H), 7.18 (d, *J* = 16.0 Hz, 1H), 7.17–7.13 (m, 1H), 7.01 (s, 1H), 6.95 (t, *J* = 8.0 Hz, 1H), 6.79 (d, *J* = 8.0 Hz, 1H), 3.90 (s, 3H), 3.89 (s, 6H); <sup>13</sup>C NMR (150 MHz, CDCl<sub>3</sub>): δ 153.1, 152.8, 150.9, 142.8, 133.2, 128.8, 128.6, 127.5, 125.2, 124.4, 121.2, 121.1, 116.0, 111.1, 105.4, 103.6, 61.2, 60.9, 56.2; HRMS  $m/z$  ( $M + 1$ )<sup>+</sup> calcd for C<sub>17</sub>H<sub>18</sub>BrO<sub>4</sub>, 365.0383; found, 365.0378.

(*E*)-2-(2-(Benzo[d][1,3]dioxol-5-yl)vinyl)-6-methoxyphenol (**31**). White solid; mp 141–143 °C; <sup>1</sup>H NMR (500 MHz, CDCl<sub>3</sub>): δ 7.23 (d, *J* = 15.0 Hz, 1H), 7.12 (dd, *J* = 8.0, 1.5 Hz, 1H), 7.09 (s, 1H), 7.08 (d, *J* = 15.0 Hz, 1H), 6.94 (dd, *J* = 8.0, 1.5 Hz, 1H), 6.82 (t, *J* = 8.0 Hz,

1H), 6.76 (d, *J* = 8.0 Hz, 1H), 6.74 (dd, *J* = 8.0, 1.5 Hz, 1H), 5.95 (s, 2H), 3.89 (s, 3H); <sup>13</sup>C NMR (125 MHz, CDCl<sub>3</sub>): δ 148.1, 147.1, 146.7, 143.3, 132.5, 129.1, 123.8, 121.4, 121.3, 119.5, 118.6, 109.2, 108.3, 105.7, 101.0, 56.1; HRMS  $m/z$  ( $M + Na$ )<sup>+</sup> calcd for C<sub>16</sub>H<sub>14</sub>O<sub>4</sub>Na, 293.0784; found, 293.0736.

(*E*)-5-(2-(Benzo[d][1,3]dioxol-5-yl)vinyl)-2-methoxyphenol (**32**). White solid; mp 139–141 °C; <sup>1</sup>H NMR (500 MHz, CDCl<sub>3</sub>): δ 7.01 (d, *J* = 19.0 Hz, 2H), 6.97 (d, *J* = 8.0 Hz, 1H), 6.91–6.84 (m, 4H), 6.77 (d, *J* = 8.0 Hz, 1H), 5.95 (s, 2H), 5.61 (s, 1H), 3.93 (s, 3H); <sup>13</sup>C NMR (125 MHz, CDCl<sub>3</sub>): δ 148.1, 147.0, 146.7, 145.4, 132.1, 130.1, 127.0, 126.2, 121.0, 120.2, 114.5, 108.4, 108.1, 105.4, 101.1, 55.9; HRMS  $m/z$  ( $M + 1$ )<sup>+</sup> calcd for C<sub>16</sub>H<sub>15</sub>O<sub>4</sub>, 271.0965; found, 271.0916.

(*E*)-5-(3,4,5-Trimethoxystyryl)benzo[d][1,3]dioxole (**33**). White solid; mp 129–131 °C; <sup>1</sup>H NMR (500 MHz, CDCl<sub>3</sub>): δ 6.77 (m, 2H), 6.69 (dd, *J* = 7.5, 0.5 Hz, 1H), 6.49 (s, 2H), 6.44 (d, *J* = 12.0 Hz, 1H), 6.39 (d, *J* = 12.0 Hz, 1H), 5.89 (s, 2H), 3.82 (s, 3H), 3.69 (s, 6H); <sup>13</sup>C NMR (125 MHz, CDCl<sub>3</sub>): δ 152.9, 147.3, 146.6, 137.2, 132.5, 131.1, 129.4, 129.1, 122.9, 109.0, 108.1, 106.0, 100.9, 60.9, 55.9; HRMS  $m/z$  ( $M + 1$ )<sup>+</sup> calcd for C<sub>18</sub>H<sub>19</sub>O<sub>5</sub>, 315.1227; found, 315.1223.

3-(3,4-Dimethoxystyryl)-4-hydroxy-5-methoxybenzaldehyde (**34**). White solid; mp 157–159 °C; <sup>1</sup>H NMR (500 MHz, CDCl<sub>3</sub>): δ 9.85 (s, 1H), 7.69 (d, *J* = 1.5 Hz, 1H), 7.28 (d, *J* = 1.5 Hz, 1H), 7.26–7.18 (m, 2H), 7.10–7.07 (m, 2H), 6.85 (d, *J* = 8.0 Hz, 1H), 6.50 (s, 1H), 3.97 (s, 3H), 3.93 (s, 3H), 3.89 (s, 3H); <sup>13</sup>C NMR (125 MHz, CDCl<sub>3</sub>): δ 191.1, 149.2, 149.1, 148.6, 147.3, 130.6, 130.4, 129.2, 124.4, 124.1, 120.2, 119.5, 111.2, 108.9, 106.9, 56.3, 55.9, 55.9; HRMS  $m/z$  ( $M + 23$ )<sup>+</sup> calcd for C<sub>18</sub>H<sub>18</sub>O<sub>5</sub>Na, 337.1046; found, 337.1042.

Ethyl (*E*)-3-(3-((*E*)-3,4-Dimethoxystyryl)-4-hydroxy-5-methoxyphenyl)acrylate (**35**). White solid; mp 171–173 °C; <sup>1</sup>H NMR (500 MHz, CDCl<sub>3</sub>): δ 7.64 (d, *J* = 16.0 Hz, 1H), 7.34 (d, *J* = 1.5 Hz, 1H), 7.22 (d, *J* = 16.5 Hz, 1H), 7.13 (d, *J* = 16.5 Hz, 1H), 7.09–7.06 (m, 2H), 6.91 (d, *J* = 1.5 Hz, 1H), 6.85 (d, *J* = 8.0 Hz, 1H), 6.32 (d, *J* = 16.0 Hz, 1H), 6.18 (br, 1H), 3.93 (s, 3H), 3.92 (s, 3H), 3.89 (s, 3H), 3.79 (s, 3H); <sup>13</sup>C NMR (125 MHz, CDCl<sub>3</sub>): δ 167.6, 149.1, 149.0, 146.9, 145.3, 145.1, 130.6, 130.1, 126.3, 124.1, 120.3, 120.1, 120.0, 115.4, 111.2, 108.9, 107.4, 56.2, 55.9, 55.9, 51.6; HRMS  $m/z$  ( $M + 1$ )<sup>+</sup> calcd for C<sub>21</sub>H<sub>23</sub>O<sub>6</sub>, 371.1489; found, 374.1488.

**Biological Procedures. Cell Culture.** Primary cultures of neonatal cortical neurons were prepared as described previously.<sup>27</sup> The Institutional Animal Care and Use Committee at the National Research Institute of Chinese Medicine approved the animal protocol. In brief, the cortex was isolated from Sprague–Dawley rat pups by decapitation and digested in 0.5 mg/mL papain at 37 °C for 15 min. The tissue was dissociated in Hibernate A medium (containing B27 supplement) by aspirating trituration. Cells were plated and maintained in Neurobasal medium containing B27 supplement, 10 units/mL penicillin, 10 μg/mL streptomycin, and 0.5 μg/mL glutamine for 3 days. Cells were then exposed to cytosine-β-D-arabino-furanoside (5 μM) for 1 day to eliminate the proliferation of non-neuronal cells. The cells were used for Aβ and glutamate experiments at days in vitro (DIV) 5 and DIV10, respectively. Neurons are vulnerable to Aβ-mediated toxicity at DIV5 and expression of glutamate receptor at DIV10. Primary mixed glial cells were prepared from the cerebral cortex and maintained in DMEM/F12 medium containing 10% FBS for 3 days. The medium was changed with fresh culture medium, and cells were incubated for 4 days. Thereafter, the cells were cultured in Neurobasal medium/B27 supplement for 9 more days.

**Preparation and Biochemical Characterization of fAβ25–35.** fAβ25–35 was prepared by dissolving Aβ25–35 in H<sub>2</sub>O at 1 mM and aging for 1 week at 37 °C. A diluted solution of Aβ was spotted onto a mica slide and scanned using an Agilent 5400 atomic microscope (Molecular Imaging Cooperation, Temp, A2) as describe previously.<sup>24</sup>

**Treatment with fAβ25–35 or Glutamate and Synthetic Compounds.** Cortical neurons were pretreated with vehicle [0.1% dimethyl sulfoxide (DMSO)] or the synthetic compounds for 30 min. Then, fAβ25–35 or glutamate was added directly into the medium and the cells were incubated for 48 or 24 h, respectively.

**Measurement of Cell Viability.** The live/dead cell viability assay and the reduction of MTT were used to evaluate cell viability. Cells were loaded with 1  $\mu$ M of both calcein AM and ethidium homodimer-1 at room temperature for 30 min. The cells were observed by confocal laser scanning microscopy (Jena, Germany). The reduction of MTT was used to evaluate cell viability. Cells were incubated with 0.5 mg/mL MTT for 1 h. The formazan particles were dissolved in DMSO. OD<sub>600 nm</sub> was measured using an enzyme-linked immunosorbent assay reader.

**Immunocytochemistry.** Treated cells were fixed with 4% paraformaldehyde at room temperature for 15 min and permeabilized with 0.5% Triton X-100 for 10 min. Cells were blocked with 10% control donkey serum at room temperature for 2 h. Thereafter, cells were exposed to anti-MAP2 monoclonal antibody (1:100, Invitrogen) or goat anti-au antibody (1:100, Santa Cruz) at 4 °C overnight. After washing, the cells were incubated in staining solution containing fluorescein isothiocyanate-conjugated donkey anti-mouse IgG and RRX-conjugated donkey anti-goat IgG (1:200; Jackson ImmunoResearch) in the dark overnight at 4 °C. Cells were then washed with PBS and mounted with Aqua Poly/Mount (Polyscience Inc., Warrington, PA, USA). The excitation/emission wavelengths used for fluorescein isothiocyanate and RRX were 488/520 and 570/590, respectively. Fluorescence intensity was quantified using MetaMorph software.

**Measurement of Nitrite.** Nitrite content (NO release) was measured by incubating culture medium with an equal volume of Griess reagent (0.05% *N*-(1-naphthyl)-ethylene-diamine dihydrochloride, 0.5% sulfanilamide, and 1.25% phosphoric acid). After incubation, the optical density was detected at a wavelength of 540 nm using a microplate reader with NaNO<sub>2</sub> as the standard.

**Cytochrome P450 3A4 (CYP3A4) Activity Assay.** The wild-type CYP3A4 constructs with N-terminal modifications were generously provided by Dr. F. Peter Guengerich (Nashville, TN, USA).<sup>29</sup> Enzyme expression and membrane preparation were performed as described before.<sup>30</sup> Cytochrome P450 content was determined using a spectral method reported by Omura and Sato.<sup>31</sup> Nifedipine oxidation activity of CYP3A4 was determined following the method reported by Guengerich et al.<sup>32</sup> The mean of 3–4 determinations of CYP3A4 activity in the presence of increasing concentrations of hydroxyl-functionalized stilbenes or 2-arylbenzo[*b*]furans was used for calculating the IC<sub>50</sub> (the concentration required for 50% inhibition of catalytic activity). IC<sub>50</sub> values were calculated by curve fitting using a Grafit software (start at 0, defined end; Erithacus Software Ltd., Staines, UK).

**Evaluation of Antioxidant Activity.** The antioxidant activity of the synthetic compounds was determined by trolox equilibrium antioxidant capacity (TEAC) as described previously.<sup>33</sup>

**Predicted Physicochemical Properties.** QikProp application was used for predicting the physicochemical properties of compounds presented in this study.<sup>34</sup>

**Animal Management and Administration.** The Institutional Animal Care and Use Committee at the National Research Institution of Chinese Medicine approved the animal protocol (IACUC nos. 100-A-04 and 102-417-3). The APP<sup>swe</sup>/PS1 $\Delta$ E9 double transgenic mouse model (APP/PS1) of AD was purchased from Jackson Laboratory (no. 005864); this mouse expresses a chimeric mouse/human APP695 harboring the Swedish K670M/N671L mutations (APP<sup>swe</sup>) and human PS1 with the exon-9 deletion mutation (PS1 $\Delta$ E9). The gender ratio for breeding was one male with two females in one cage. Experiments were conducted using WT siblings and AD transgenic female C57BL/6J mice. The animals were housed under controlled temperature (24  $\pm$  1 °C) and humidity (55–65%) with a 12:12 h (07:00–19:00) light–dark cycle. All mice were provided with commercially available rodent normal chow diet and water ad libitum. To explore the effects of the synthetic compounds in vivo, 5 month old APP/PS1 mice were fed with the synthetic compounds (30 mg/kg/day) and examined using behavioral tests.

**Nesting Test.** After oral gavage administration for 60 days, the nesting ability of the mice was assessed as described previously.<sup>35,36</sup> Two nestlets (approximately 5 g) were placed into cage at 1 h before the dark cycle, and then the nest score and the weight of unshredded

nestlets were determined after an overnight period. The nest quality was assessed on a 1–5 rating scale, with 1 indicating that the nestlet was not noticeably touched, 2 indicating that the nestlet was partially shredded and scattered on the floor, 3 indicating that the nestlet was mostly shredded but only a flat nest was built, 4 indicating that the nest was identifiable but flat, and 5 indicating that the nest was built in a burrow.

**Statistical Analysis.** The results are expressed as the mean  $\pm$  standard error of the mean (SEM) and were analyzed by analysis of variance (ANOVA) with post hoc Bonferroni multiple comparison tests.

## ■ ASSOCIATED CONTENT

### 📄 Supporting Information

The Supporting Information is available free of charge on the ACS Publications website at DOI: 10.1021/acs.jmedchem.7b00376.

Cell toxicity assay results for compounds 4, 5, and 11–43 on cortical neurons and mixed glial culture; <sup>1</sup>H and <sup>13</sup>C NMR spectra of compounds 4, 9, and 11–35 (PDF)

Molecular formula strings (CSV)

## ■ AUTHOR INFORMATION

### Corresponding Authors

\*E-mail: yshiao@nricm.edu.tw. Phone: 886-2-2820-1999 ext. 4163 (Y.-J.S.).

\*E-mail: wtli@nricm.edu.tw. Phone: 886-2-2820-1999 ext. 8261 (W.-T.L.).

### ORCID

Wen-Tai Li: 0000-0002-7610-1778

### Author Contributions

<sup>§</sup>Y.-J.S. and W.-T.L. contributed equally to this work.

### Notes

The authors declare no competing financial interest.

## ■ ACKNOWLEDGMENTS

This study was supported by the Ministry of Science and Technology (MOST 103-2320-B-077-004-MY3; MM10501-0274).

## ■ ABBREVIATIONS USED

A $\beta$ ,  $\beta$ -amyloid peptide; AD, Alzheimer's disease; APP/PS1, APP<sup>swe</sup>/PS1 $\Delta$ E9; ADL, activities of daily living; DCM, dichloromethane; DMSO, dimethyl sulfoxide; EthD-1, ethidium homodimer-1; MAP2, microtubule associated protein 2; MTT, 3-(4,5-dimethylthiazol-2-yl)-2,5-diphenyltetrazolium bromide; NFT, neurofibrillary tangle; ROS, reactive oxygen species; NMDA, *N*-methyl-D-aspartate; NO, nitric oxide; TAB, tournefolic acid B; TABM, tournefolic acid B methyl ester; WT, wild type

## ■ REFERENCES

- (1) Hardy, J.; Selkoe, D. J. The amyloid hypothesis of Alzheimer's disease: progress and problems on the road to therapeutics. *Science* **2002**, *297*, 353–356.
- (2) Selkoe, D. J. Clearing the brain's amyloid cobwebs. *Neuron* **2001**, *32*, 177–180.
- (3) Echeverria, V.; Yarkov, A.; Aliev, G. Positive modulators of the  $\alpha$ 7 nicotinic receptor against neuroinflammation and cognitive impairment in Alzheimer's disease. *Prog. Neurobiol.* **2016**, *144*, 142–157.
- (4) Sierra, A.; Beccari, S.; Diaz-Aparicio, I.; Encinas, J. M.; Comeau, S.; Tremblay, M. E. Surveillance, phagocytosis, and inflammation: how never-resting microglia influence adult hippocampal neurogenesis. *Neural Plast.* **2014**, *2014*, 610343.

- (5) Rosini, M.; Simoni, E.; Minarini, A.; Melchiorre, C. Multi-target design strategies in the context of Alzheimer's disease: acetylcholinesterase inhibition and NMDA receptor antagonism as the driving forces. *Neurochem. Res.* **2014**, *39*, 1914–1923.
- (6) Chiang, K.; Koo, E. H. Emerging therapeutics for Alzheimer's disease. *Annu. Rev. Pharmacol. Toxicol.* **2014**, *54*, 381–405.
- (7) Awasthi, M.; Singh, S.; Pandey, V. P.; Dwivedi, U. N. Alzheimer's disease: An overview of amyloid beta dependent pathogenesis and its therapeutic implications along with in silico approaches emphasizing the role of natural products. *J. Neurol. Sci.* **2016**, *361*, 256–271.
- (8) Chang, Y. T.; Chang, W. N.; Tsai, N. W.; Huang, C. C.; Kung, C. T.; Su, Y. J.; Lin, W. C.; Cheng, B. C.; Su, C. M.; Chiang, Y. F.; Lu, C. H. The roles of biomarkers of oxidative stress and antioxidant in Alzheimer's disease: a systematic review. *BioMed Res. Int.* **2014**, *2014*, 182303.
- (9) Eskici, G.; Axelsen, P. H. Copper and oxidative stress in the pathogenesis of Alzheimer's disease. *Biochemistry* **2012**, *51*, 6289–6311.
- (10) Lin, Y. L.; Chang, Y. Y.; Kuo, Y. H.; Shiao, M. S. Anti-lipid-peroxidative principles from *Tournefortia sarmentosa*. *J. Nat. Prod.* **2002**, *65*, 745–747.
- (11) Wang, C. N.; Pan, H. C.; Lin, Y. L.; Chi, C. W.; Shiao, Y. J. Ester derivatives of tournefoliac acid B attenuate *N*-methyl-D-aspartate-mediated excitotoxicity in rat cortical neurons. *Mol. Pharmacol.* **2006**, *69*, 950–959.
- (12) Chi, C. W.; Wang, C. N.; Lin, Y. L.; Chen, C. F.; Shiao, Y. J. Tournefoliac acid B methyl ester attenuates glutamate-induced toxicity by blockade of ROS accumulation and abrogating the activation of caspases and JNK in rat cortical neurons. *J. Neurochem.* **2005**, *92*, 692–700.
- (13) Chi, C. W.; Lin, Y. L.; Wang, Y. H.; Chen, C. F.; Wang, C. N.; Shiao, Y. J. Tournefoliac acid B attenuates amyloid beta protein-mediated toxicity by abrogating the calcium overload in mitochondria and retarding the caspase 8-truncated Bid-cytochrome c pathway in rat cortical neurons. *Eur. J. Pharmacol.* **2008**, *586*, 35–44.
- (14) Lin, Y. L.; Tsay, H. J.; Lai, T. H.; Tzeng, T. T.; Shiao, Y. J. Lithospermic acid attenuates 1-methyl-4-phenylpyridine-induced neurotoxicity by blocking neuronal apoptotic and neuroinflammatory pathways. *J. Biomed. Sci.* **2015**, *22*, 37.
- (15) Ma, T.; Tan, M. S.; Yu, J. T.; Tan, L. Resveratrol as a therapeutic agent for Alzheimer's disease. *BioMed Res. Int.* **2014**, *2014*, 350516.
- (16) Tellone, E.; Galtieri, A.; Russo, A.; Giardina, B.; Ficarra, S. Resveratrol: A Focus on Several Neurodegenerative Diseases. *Oxid. Med. Cell. Longevity* **2015**, *2015*, 392169.
- (17) Malhotra, A.; Bath, S.; Elbarbry, F. An Organ System Approach to Explore the Antioxidative, anti-Inflammatory, and cytoprotective actions of resveratrol. *Oxid. Med. Cell. Longevity* **2015**, *2015*, 803971.
- (18) Choi, D. K.; Koppula, S.; Suk, K. Inhibitors of microglial neurotoxicity: focus on natural products. *Molecules* **2011**, *16*, 1021–1043.
- (19) Rizzo, S.; Tarozzi, A.; Bartolini, M.; Da Costa, G.; Bisi, A.; Gobbi, S.; Belluti, F.; Ligresti, A.; Allarà, M.; Monti, J. P.; Andrisano, V.; Di Marzo, V.; Hrelia, P.; Rampa, A. 2-Arylbenzofuran-based molecules as multipotent Alzheimer's disease modifying agents. *Eur. J. Med. Chem.* **2012**, *58*, 519–532.
- (20) Nassra, M.; Krisa, S.; Papastamoulis, Y.; Kapche, G. D.; Bisson, J.; André, C.; Konsman, J. P.; Schmitter, J. M.; Méryllon, J. M.; Waffo-Téguo, P. Inhibitory activity of plant stilbenoids against nitric oxide production by lipopolysaccharide-activated microglia. *Planta Med.* **2013**, *79*, 966–970.
- (21) Hsieh, J. F.; Lin, W. J.; Huang, K. F.; Liao, J. H.; Don, M. J.; Shen, C. C.; Shiao, Y. J.; Li, W. T. Antioxidant activity and inhibition of  $\alpha$ -glucosidase by hydroxyl-functionalized 2-arylbenzo[b]furans. *Eur. J. Med. Chem.* **2015**, *93*, 443–451.
- (22) Reinisalo, M.; Karlund, A.; Koskela, A.; Kaarniranta, K.; Karjalainen, R. O. Polyphenol stilbenes: molecular mechanisms of defence against oxidative stress and aging-related diseases. *Oxid. Med. Cell. Longevity* **2015**, *2015*, 340520.
- (23) Das, J.; Pany, S.; Majhi, A. Chemical modifications of resveratrol for improved protein kinase C alpha activity. *Bioorg. Med. Chem.* **2011**, *19*, 5321–5324.
- (24) Tsay, H. J.; Huang, Y. C.; Huang, F. L.; Chen, C. P.; Tsai, Y. C.; Wang, Y. H.; Wu, M. F.; Chiang, F. Y.; Shiao, Y. J. Amyloid  $\beta$  peptide-mediated neurotoxicity is attenuated by the proliferating microglia more potently than by the quiescent phenotype. *J. Biomed. Sci.* **2013**, *20*, 78.
- (25) Nakamura, Y. Regulating factors for microglial activation. *Biol. Pharm. Bull.* **2002**, *25*, 945–953.
- (26) Kierdorf, K.; Prinz, M. Factors regulating microglia activation. *Front. Cell. Neurosci.* **2013**, *7*, 44.
- (27) Wenzel, E.; Somoza, V. Metabolism and bioavailability of trans-resveratrol. *Mol. Nutr. Food Res.* **2005**, *49*, 472–481.
- (28) Wang, C. N.; Chi, C. W.; Lin, Y. L.; Chen, C. F.; Shiao, Y. J. The neuroprotective effects of phytoestrogens on amyloid beta protein-induced toxicity are mediated by abrogating the activation of caspase cascade in rat cortical neurons. *J. Biol. Chem.* **2001**, *276*, 5287–5295.
- (29) Parikh, A.; Gillam, E. M. J.; Guengerich, F. P. Drug metabolism by *Escherichia coli* expressing human cytochrome P450. *Nat. Biotechnol.* **1997**, *15*, 784–788.
- (30) Ueng, Y. F.; Chen, C. C.; Yamazaki, H.; Kiyotani, K.; Chang, Y. P.; Lo, W. S.; Li, D. T.; Tsai, P. L. Mechanism-based inhibition of CYP1A1 and CYP3A4 by the furanocoumarin chalepensis. *Drug Metab. Pharmacokinet.* **2013**, *28*, 229–238.
- (31) Omura, T.; Sato, R. The carbon monoxide-binding pigment of liver microsomes. Evidence for its heme protein nature. *J. Biol. Chem.* **1964**, *239*, 2370–2378.
- (32) Guengerich, F. P.; Martin, M. V.; Beaune, P. H.; Kremers, P.; Wolff, T.; Waxman, D. V. Characterization of rat and human liver microsomal cytochrome P-450 forms involved in nifedipine oxidation, a prototype for genetic polymorphism in oxidative drug metabolism. *J. Biol. Chem.* **1986**, *261*, 5051–5060.
- (33) Re, R.; Pellegrini, N.; Proteggente, A.; Pannala, A.; Yang, M.; Rice-Evans, C. Antioxidant activity applying an improved ABTS radical cation decolorization assay. *Free Radical Biol. Med.* **1999**, *26*, 1231–1237.
- (34) *QikProp*, version 3.5; Schrödinger, LLC: New York, 2012.
- (35) Salloway, S.; Mintzer, J.; Weiner, M. F.; Cummings, J. L. Disease-modifying therapies in Alzheimer's disease. *Alzheimer's Dementia* **2008**, *4*, 65–79.
- (36) Yeh, C. W.; Yeh, S. H.; Shie, F. S.; Lai, W. S.; Liu, H. K.; Tzeng, T. T.; Tsay, H. J.; Shiao, Y. J. Impaired cognition and cerebral glucose regulation are associated with astrocyte activation in the parenchyma of metabolically stressed APP<sup>sw</sup>/PS1<sup>de9</sup> mice. *Neurobiol. Aging* **2015**, *36*, 2984–2994.